

2025

The role of iron in translational regulation

<https://hdl.handle.net/2144/52083>

"Downloaded from OpenBU. Boston University's institutional repository."

BOSTON UNIVERSITY

ARAM V. CHOBANIAN & EDWARD AVEDISIAN SCHOOL OF MEDICINE

Dissertation

THE ROLE OF IRON IN TRANSLATIONAL REGULATION

by

HANNA BARLIT

M.D., Odessa National Medical University, 2017
M.S., Odessa I.I. Mechnikov National University, 2019

Submitted in partial fulfillment of the

requirements for the degree of

Doctor of Philosophy

2025

© 2025 by
HANNA BARLIT
All rights reserved

Approved by

First Reader

Vyacheslav M. Labunskyy, Ph.D.
Associate Professor of Dermatology

Second Reader

Shawn Lyons, Ph.D.
Assistant Professor of Biochemistry

ACKNOWLEDGMENTS

I would like to express my strongest gratitude to my advisor, Dr. Vyacheslav Labunskyy, for his constant support, encouragement, and mentorship throughout my Ph.D. journey. I am also immensely thankful to Dr. Shoumita Dasgupta, director of the Genetics and Genomics Program, for her responsiveness and guidance in helping me navigate the challenges of graduate school. My sincere gratitude goes to the chair of my Advisory Committee, Dr. Alla Grishok, and all committee members, Dr. Shawn Lyons, Dr. Vladimir Botchkarev, and Dr. Daniel Cifuentes, for their valuable scientific insights, fruitful discussions, and assistance throughout this journey. I am deeply grateful to my lab members, including Dr. Praveen Patnaik and Tanya Labunska, whose willingness to share their expertise and patience created a welcoming and collaborative atmosphere in the lab. I also thank our collaborators for their contributions, which significantly enriched this work. Finally, I want to thank my friends and family, who have been a constant source of support and motivation.

THE ROLE OF IRON IN TRANSLATIONAL REGULATION

HANNA BARLIT

Boston University Aram V. Chobanian & Edward Avedisian School of Medicine, 2025

Major Professor: Vyacheslav M. Labunskyy, Ph.D. Associate Professor of Dermatology

ABSTRACT

Iron is an essential microelement that functions as a co-factor for enzymes involved in numerous biological processes, including mitochondrial function, DNA replication and repair, electron transport, lipid β -oxidation, and protein translation. Dysregulation of iron metabolism is a hallmark of aging and has been implicated in the development of a wide range of human age-related diseases. However, whether targeting iron homeostasis can be used to promote longer lifespan remains unclear.

In this study, we characterized the role of iron homeostasis in regulation of protein translation and its effects on aging, using *Saccharomyces cerevisiae* as a model organism. We employed genome-wide transcriptome analysis (RNA-Seq) and ribosome profiling to quantify age-dependent changes in transcription and protein translation during replicative lifespan in yeast. Our data revealed that aging in yeast was associated with an up-regulation of genes involved in iron import into the cell, whereas deletion of several members of the iron regulon led to increased longevity. We further demonstrated that defects in the conserved mRNA-binding protein Cth2, which regulates the stability and translation of mRNAs encoding iron-dependent proteins, extended lifespan by alleviating its repressive effects on mitochondrial function.

Additionally, we investigated the effect of iron depletion on protein translation. Our findings uncovered a complex effect of iron deficiency on the regulation of protein synthesis showing how this important nutrient affects protein translation through multiple mechanisms. Specifically, we found that low iron leads to specific downregulation of genes involved in iron-dependent processes, including mitochondrial translation and heme biosynthesis, at the translation level via the activation of Cth1/2. We further showed that iron deficiency affects global protein translation by decreasing the activity of the ribosome recycling factor Rli1. Finally, we identified a novel regulatory mechanism involving antisense long non-coding RNAs, which are activated under iron-depleted conditions to modulate protein translation.

Together, these findings deepened our understanding of how iron regulates protein translation and revealed Cth2 as a promising target for interventions aimed at extending lifespan.

TABLE OF CONTENTS

ACKNOWLEDGMENTS	iv
ABSTRACT.....	v
TABLE OF CONTENTS.....	vii
LIST OF TABLES	ix
LIST OF FIGURES	x
CHAPTER 1	1
Introduction.....	1
1.1. Iron: Its Molecular Biology and Role in Living Organisms	1
1.2. Iron Regulatory Mechanisms in <i>Saccharomyces cerevisiae</i>	4
1.3. Regulation of Iron Metabolism in Mammals.....	6
1.4. The Role of Iron Homeostasis in Aging	9
CHAPTER 2	12
Deficiency of the RNA-binding Protein Cth2 Extends Yeast Replicative Lifespan by Alleviating its Repressive Effects on Mitochondrial Function.....	12
2.1. Abstract.....	12
2.2. Introduction.....	12
2.3. Results.....	15
2.4. Discussion.....	28
2.5. Methods	33
CHAPTER 3	39

Ribosome Profiling Reveals the Role of Yeast RNA-binding Proteins Cth1 and Cth2 in Translational Regulation.....	39
3.1. Abstract.....	39
3.2. Introduction.....	39
3.3. Results.....	42
3.4. Discussion.....	60
3.5. Methods	65
CHAPTER 4	71
Conclusions and Future Directions.....	71
4.1. Conclusions.....	71
4.2. Future Directions	74
Supplemental Tables.....	75
List of Journal Abbreviations.....	92
BIBLIOGRAPHY.....	95
CURRICULUM VITAE.....	104

LIST OF TABLES

Table 1. Statistical analysis of lifespan experiments.	75
Table 2. Location of putative AU-rich elements (AREs) and Puf3 binding sites in genes translationally regulated by yeast Cth1/Cth2 proteins in response to Fe deficiency, related to Figure 2.	77

LIST OF FIGURES

Figure 1. Deletion of genes involved in Fe homeostasis differentially affects lifespan and cell fitness.	16
Figure 2. Deletion of genes involved in Fe metabolism differentially affects cell fitness.	17
Figure 3. Aging leads to a global inhibition of translation, but an up-regulation of genes involved in Fe homeostasis.	19
Figure 4. Comparison of ribosome occupancy changes during aging.	22
Figure 5. Constitutive activation of the Aft1 negatively regulates yeast lifespan.	23
Figure 6. Cth2 is a negative regulator of lifespan and mitochondrial respiration.	26
Figure 7. Model showing the role of Cth2 in age-related repression of mitochondrial function.	32
Figure 8. Heatmaps of Pearson correlation coefficients for RNA-Seq and Ribo-Seq replicates in wild-type cells and the <i>cth1Δcth2Δ</i> mutant in response to Fe deficiency.	43
Figure 9. Coordinated changes in mRNA levels and translation allow metabolic reprogramming in response to low Fe	44
Figure 10. Heatmaps of log ₂ fold changes in protein translation (Ribo-Seq) of Fe regulon genes during prolonged (6 h) Fe deficiency in wild-type (WT) cells and the <i>cth1Δcth2Δ</i> mutant (Mut) (FDR<0.05).	46
Figure 11. Fe deficiency leads to Cth1/2-dependent inhibition of mitochondrial translation.	48

Figure 12. Genes derepressed in <i>cth1Δcth2Δ</i> compared to wild-type cells during 6 hours of Fe deficiency.....	49
Figure 13. Heatmaps of log ₂ fold changes in protein translation (Ribo-Seq) of differentially regulated genes of the TCA cycle during short-term (3 h) and prolonged (6 h) Fe deficiency in wild-type (WT) cells and the <i>cth1Δcth2Δ</i> mutant (Mut) (FDR<0.05).....	50
Figure 14. Fe deficiency does not affect transcription levels of mitochondrial ribosomal proteins.....	51
Figure 15. Expression of the mitochondrial ribosomal proteins of the small subunit (A) and large subunit (B) during the shift from the fermentable to non-fermentable carbon source.	52
Figure 16. Heme biosynthesis is translationally regulated by Cth1 and Cth2.	53
Figure 17. Changes in Ribosome Occupancy (RO) of 3'UTR upon 6 hours of Fe deficiency.....	55
Figure 18. Fe deficiency leads to increased translation of 3'UTRs due to Cth1/2-dependent inhibition of Rli1 activity.	56
Figure 19. Fe deficiency induces expression of regulatory lncRNAs.	58
Figure 20. Expression of antisense lncRNA is a conserved regulatory mechanism in yeast.	59
Figure 21. Model for the role of yeast RNA-binding proteins Cth1 and Cth2 in the control of protein translation during adaptation to Fe deficiency.	64

CHAPTER 1

Introduction

1.1. Iron: Its Molecular Biology and Role in Living Organisms

Iron is an essential microelement required by all living organisms. Due to the high chemical reactivity of free iron, in cells iron is predominantly found in protein-bound complexes. Iron-containing proteins can be categorized into three main classes based on the structure of their iron-containing cofactors: proteins with a single iron ion, iron-sulfur (Fe/S) cluster proteins, and heme proteins [1]. These iron-dependent proteins function in a diverse array of enzymatic reactions that regulate essential metabolic processes, including DNA synthesis and repair, mitochondrial respiration, lipid β -oxidation, and protein synthesis.

Iron distribution within the cell is heterogeneous and varies across subcellular compartments. Recent analyses of the human proteome identified 398 iron-binding proteins [1]. Of these, 139 bind a single metal ion, 192 bind heme, and 70 are Fe/S cluster proteins. Among subcellular compartments, mitochondria and the endoplasmic reticulum each contain approximately 7% of all iron-containing proteins. Notably, mitochondria are enriched in Fe/S proteins, while the endoplasmic reticulum predominantly contains heme-binding proteins. In contrast, the nucleus is enriched in single-ion iron-binding proteins, which are critical for DNA synthesis and repair [1].

In the endoplasmic reticulum, the majority of iron-binding proteins function as oxidoreductases, including cytochromes P450, which contain heme, and iron-dependent

hydroxylases that typically possess two iron ions in their active sites. These enzymes play important roles in lipid metabolism and detoxification of xenobiotics and drugs.

The enrichment of mitochondria with Fe/S cluster proteins not only reflects their crucial role in synthesis of Fe/S clusters but also the fact that the mitochondrial function itself heavily depends on iron-containing proteins. Iron plays a pivotal role in the electron transport chain (ETC), where Fe/S clusters and heme groups mediate the redox reactions that drive the transfer of electrons through the complexes (Complex I, II, III, IV, and c) [2]. In addition to the key role of Fe/S proteins in the electron transport chain, Fe/S cluster proteins regulate diverse processes, including apoptosis, iron ion homeostasis, and responses to oxidative stress.

In the nucleus, numerous enzymes such as helicases, nucleases, glycosylases, demethylases, and ribonucleotide reductases, require iron for their catalytic activity. Additionally, recent findings show that the catalytic subunits of DNA polymerases in the nucleus contain conserved cysteine-rich motifs that coordinate Fe/S clusters. These clusters are essential for the formation of stable and active enzyme complexes, ensuring accurate DNA replication and repair processes within the nuclear environment [3].

Iron also plays a fundamental role in protein biosynthesis, intersecting with various stages of protein translation. Specifically, Fe/S clusters are required for the biosynthesis of amino acids such as valine, leucine, and isoleucine. Additionally, intracellular cysteine levels are closely linked to ferroptosis activation, underscoring the complex interplay between iron and cellular metabolic processes [4, 5]. During peptide elongation, Fe/S clusters are required for wybutosine modifications of tRNAs, a critical enzymatic reaction

for proper protein translation. Ribosome recycling, which ensures efficient protein translation termination, depends on Rli1, and Fe/S cluster-containing ribosome recycling factor (ABCE1 in mammalian cells) [6]. In this study, we explored the effects of iron deficiency on global protein translation, focusing on Rli1 function. These results will be discussed in Chapter 3.

Another iron-dependent process involves diphthamide synthesis and diphthamide modification of the translation elongation factor eIF2a by Dph1-Dph7. Ribosome profiling revealed impaired translation elongation, frame-shifting, and premature translation termination in yeast and mammalian cells lacking diphthamide [7]. In this study, we report a novel mechanism of Dph1 translation regulation during iron deficiency.

To support all the chemical reactions discussed, iron homeostasis has evolved into a highly dynamic system involving multiple regulatory levels, including iron utilization, storage, incorporation into proteins, and recycling. The complexity of iron regulation arises not only from the diversity of iron-dependent processes but also from iron's low bioavailability and high chemical reactivity [8].

Interestingly, the evolution of multicellular life coincided with the oxygenation of Earth's atmosphere, which resulted in an abrupt decrease in iron bioavailability for all living organisms. As a result, organisms with efficient iron acquisition and recycling were evolutionarily favored. Modern multicellular organisms rely primarily on recycling iron within the organism, particularly through processing senescent cells, rather than external iron sources, enabling greater adaptability under conditions with limited iron availability [9].

In the following section, we discuss the regulation of iron metabolism in *Saccharomyces cerevisiae*, a single-cell eukaryotic model organism central to the experiments presented in Chapters 2 and 3.

1.2. Iron Regulatory Mechanisms in *Saccharomyces cerevisiae*

Previous studies in *Saccharomyces cerevisiae* have shown that iron-deficiency induces substantial changes in gene expression, predominantly mediated by the Aft1 and Aft2 transcription factors. Under conditions of iron-scarcity, Aft1 and Aft2 translocate to the nucleus, where they activate the transcription of genes responsible for increased iron acquisition (*ARN1*, *ARN2*, *ARN3*, *ARN4*, *FIT1*, *FIT2*, and *FIT3*), mobilization of intracellular iron stores (*FTH1*), and heme degradation (*HMX1*), thereby compensating for limited iron availability [10]. Additionally, Aft1 induces the expression of mRNA-binding protein Cth2 and its paralog Cth1. These proteins recognize AU-rich elements (AREs) in the 3' untranslated regions (UTRs) of mRNAs encoding non-essential iron-containing proteins. By promoting degradation of these mRNAs, Cth1 and Cth2 facilitate the reallocation of iron to essential processes, such as DNA synthesis and repair, which require Fe/S cluster-containing enzymes like DNA polymerases and helicases [11, 12].

In yeast, Fe/S clusters-containing proteins Grx3 and Grx4 serve as sensors of intracellular iron levels, modulating activity of the Aft1 transcription factor. Notably, deletion of several genes involved in regulation of iron homeostasis, including *CTH2*, *CTH1*, *FET3*, *HMX1*, and *FIT2* has been associated with lifespan extension [13].

In this work, we discovered that aging in yeast is tightly associated with the increased expression of genes involved in iron homeostasis. We further demonstrated that aberrant expression of Cth2 in aged yeast cells limits replicative lifespan by repressing mitochondrial function. These data will be discussed in detail in Chapter 2.

Although the transcriptional response to iron deficiency has been extensively characterized, many of the genes can be also regulated at the level of protein translation. In Chapter 3, we explored the genome-wide response to iron depletion at the translational level and examined the role of Cth2 in remodeling iron metabolism. We discovered a novel mechanism of translation regulation mediated by long non-coding RNAs (lncRNAs) activated under iron-deficient conditions. Notably, these lncRNAs influence translation of proteins critical for iron-associated processes, such as mitochondrial iron transport via Mrs3 and diphthamide biosynthesis mediated by Dph1.

Additionally, we identified previously uncharacterized targets of Cth2 that are affected at the level of translation. Specifically, Cth2 suppresses the translation of genes involved in heme biosynthesis (*HEM1*, *HEM3*, *HEM12*, *HEM15*), resulting in a significant reduction in intracellular heme levels. In contrast, heme levels remained unchanged in *cth2Δ* cells, even under iron depletion conditions. These findings enhance our understanding of Cth2's role in remodeling iron metabolism under iron-restricted conditions.

Previous studies demonstrated that, in response to iron deficiency, Cth2 downregulates *RLII*, which encodes the ribosome recycling factor. In this study, we showed that even after prolonged iron deficiency (6 hours), yeast cells retain sufficient iron

to sustain Rli1 function when *CTH2* is knocked out. This observation led us to conclude that Cth2's role extends beyond the degradation of mRNA encoding non-essential iron-containing proteins when iron availability is insufficient for their function. Instead, Cth2 also restricts the distribution of iron, even when intracellular iron levels remain adequate.

1.3. Regulation of Iron Metabolism in Mammals

Regulation of iron homeostasis in mammals is more complex compared to yeast. Drawing parallels between the activation of iron-regulated genes in these systems, the function of Aft1 and Aft2 can be viewed as analogous to mammalian iron regulatory proteins (IRP1 and IRP2), as both are activated in response to iron deficiency. However, there is a key difference: in yeast, iron-regulated genes are upregulated at the transcriptional level, whereas in mammals, this regulation occurs post-transcriptionally.

In mammals, iron absorption occurs in the apical part of enterocytes lining the small intestine, either in the form of metal ions or heme, via distinct transporter systems. Iron bioavailability—the fraction of dietary iron absorbed—depends on factors such as diet composition, intestinal health, food type, and processing time. Pathological conditions affecting the gastrointestinal system can impair iron absorption, leading to iron deficiency. Notably, mammals lack a regulated mechanism for controlled iron excretion, making iron import, distribution, and recycling critical for maintaining iron homeostasis.

Iron absorption begins with the reduction of ferric iron Fe^{3+} to ferrous iron Fe^{2+} by the ferric reductase enzyme, duodenal cytochrome b1 (Dcytb). Fe^{2+} is then imported into enterocytes via the divalent metal transporter 1 (DMT1), where it binds to ferritin for

storage. A portion of ferritin-bound iron remains within enterocytes, while the remainder is distributed throughout the organism. For distribution, Fe^{2+} is reoxidized to Fe^{3+} by ferroxidases such as hephaestin or ceruloplasmin (encoded by the *HEPH* and *CP* genes, respectively), and exported through ferroportin, the sole known iron exporter in mammals (encoded by the *SLC40A1* gene in humans). Once in circulation, Fe^{3+} binds to transferrin, the primary plasma iron transporter and an important clinical marker for systemic iron deficiency. Cellular iron uptake is mediated by the transferrin receptor 1 (TFR1), which binds transferrin and facilitates iron internalization.

In mammalian cells, intracellular iron homeostasis is governed by IRP1 and IRP2. Under iron-replete conditions, IRP1 functions as a cytosolic aconitase, while IRP2 is degraded by the iron-sensing ubiquitin ligase FBXL5. In iron-deficient conditions, IRP1 becomes activated through the loss of its Fe/S cluster (ISC), while IRP2 is stabilized. Both IRP1 and IRP2 bind iron regulatory elements (IREs) in the 5' and 3' untranslated regions (UTRs) of target mRNAs, regulating their translation and stability. For example, under iron deficiency, IRPs enhance the translation of transferrin receptor (*TFR1*) to increase iron uptake while suppressing the translation of ferritin (*FT*) and ferroportin (*FPN*) to limit iron export and storage. Simultaneously, iron scarcity activates heme degradation via heme oxygenase 1 (*HMOX1*), releasing iron from heme stores. Notably, the majority of daily iron needs (approximately 10-25 mg/day) are met through macrophage-mediated recycling of senescent red blood cells [14].

At the systemic level, hepcidin, a peptide hormone encoded by *HAMP*, is the master regulator of iron metabolism. Hepcidin binds to ferroportin, inducing its internalization and

degradation, thereby inhibiting iron export from storage cells into the bloodstream. By this, hepcidin coordinates circulating iron levels with physiological needs, responding to conditions such as inflammation, plasma iron concentration, hypoxia, and erythropoiesis.

Hepcidin is transcriptionally upregulated via the BMP-SMAD4 signaling pathway in response to elevated iron levels or inflammation. BMP2 and BMP6, ligands for BMP receptors on the surface of hepatocytes, initiate a signaling cascade through phosphorylation of SMAD1, SMAD5, and SMAD8. Phosphorylated SMAD1/5/8 then form a complex with SMAD4, translocate to the nucleus, and promote transcription of hepcidin. While BMP6 expression is upregulated by high iron levels, BMP2 has a higher basal expression but is less iron-sensitive. During inflammatory response, interleukin-6 (IL6) increases hepcidin expression through activation of JAK2-STAT3 signaling, promoting iron sequestration in macrophages to limit pathogen access to iron.

Another pathway for hepcidin activation involves transferrin and its receptor, transferrin receptor 2 (TFR2). Unlike the ubiquitously expressed TFR1, TFR2 is primarily found in hepatocytes and erythroblasts and has a lower transferrin-binding affinity. Elevated plasma iron levels increase transferrin binding to TFR2, upregulating hepcidin in hepatocytes. This dual role of transferrin as both an iron transporter and regulatory molecule highlights its significance in iron homeostasis. Notably, mutations in the *TFR1* receptor have been associated with impaired T- and B-lymphocyte development, leading to immunodeficiency [15].

Hepcidin expression is negatively regulated by transmembrane serine protease 6 (TMPRSS6) in response to increased iron demand during iron deficiency, active

erythropoiesis, and hypoxia. *TMPRSS6* cleaves and inactivates hemojuvelin (HJV), a BMP-SMAD pathway co-receptor. This proteolytic activity is a key mechanism by which *TMPRSS6* suppresses hepcidin levels to increase iron availability. Mutations in *TMPRSS6* result in iron-refractory iron deficiency anemia (IRIDA) [16, 17].

In mammals, the mRNA-binding protein tristetraprolin (TTP, ZFP36) is a homolog of yeast Cth2 and plays an important regulatory role in iron homeostasis. TTP binds to AU-rich elements (AREs) in the 3' untranslated regions (UTRs) of mRNAs encoding non-essential iron-containing proteins, facilitating their degradation to conserve iron for essential cellular functions [18-20]. Interestingly, TTP is activated by pathways independent of IRP1/2, such as mTOR signaling, and can counteract IRP1/2-mediated response by destabilizing *TFR1* mRNA [18]. In this study, we characterized the role of Cth2, the yeast homolog of TTP, in translational regulation and the iron deficiency response. Our findings provide a strong foundation for translating insights from yeast to mammalian systems, deepening our understanding of conserved mechanisms governing iron metabolism.

1.4. The Role of Iron Homeostasis in Aging

Iron deficiency encompasses a broad category of iron metabolism disorders and represents the most prevalent nutritional deficiency worldwide, often leading to iron deficient anemia. Older populations are particularly vulnerable to iron deficiency due to various factors, including impaired iron absorption, diminished liver function, internal bleeding, chronic kidney diseases, and persistent inflammation [14, 21]. Conversely,

excessive iron accumulation in neurons is a hallmark of age-associated neurodegenerative diseases such as Alzheimer's disease, Parkinson's disease, and multiple system atrophy (MSA). However, precise mechanisms underlying this iron accumulation and whether it is cause or consequence of these diseases remain unclear [22].

Currently, therapeutic strategies for manipulating iron levels are limited. Patients with iron overload typically undergo phlebotomy, a process that removes iron-saturated blood from circulation. While this alleviates symptoms, it does not address the underlying cause of iron overload. Another common approach to deal with iron overload is a chelation therapy, which involves the intravenous administration of iron chelators such as ethylenediaminetetraacetic acid (EDTA). These chelators bind metal ions for excretion but can result in serious side effects, including arrhythmia, seizures, and damage to the kidneys and liver. Given these drawbacks, particularly for older patients, these approaches are far from optimal.

Iron deficiency can result from malnutrition, malabsorption, blood loss, or cancer [23]. Clinically, iron deficiency is characterized by low hemoglobin level, low serum iron, reduced serum ferritin, decreased transferrin saturation, and elevated total binding capacity of transferrin [24, 25]. These conditions often manifest as iron deficient anemia, traditionally managed with oral iron supplements in conjunction with dietary modifications. Despite the widespread use of oral iron supplements, well-designed clinical trials, including placebo-controlled studies, are limited in demonstrating their efficacy. Intravenous iron administration has proven more effective in older patients, bypassing malabsorption issues, though it remains associated with venesection-related complications.

Notably, most studies evaluating treatment efficacy focus on hematological improvements rather than symptom relief or enhanced physical performance [25-28].

As we discussed above, dysregulation of iron metabolism in elderly is a result of multiple factors and occurs in a system with exhausted compensatory mechanisms. Current therapeutic approaches primarily address a single variable in the complex equation of iron homeostasis – serum iron concentration. This focus may be insufficient given the intricate mechanisms controlling iron distribution and utilization by the cell. Analysis of the literature has revealed significant gaps in our understanding of cellular responses to iron deficiency in humans. Advances in modern sequencing technologies now allow us to examine these responses at transcriptional, translational, metabolomic, and epigenetic levels, even at single cell resolution.

In this study, we sought to address key questions regarding the impact of disrupted metabolism in aging cells: What are the effects of iron dysregulation in aging cells? Do aged cells replicate the transcriptional and translational patterns observed under iron deficiency? And if so, can these patterns be reversed in aging cells? To investigate these questions, we utilized yeast as a model organism for its simplicity and employed RNA sequencing (RNA-seq) and ribosome profiling to analyze the cellular response to iron deficiency. Our study provides detailed regulatory and mechanistic insights and lay the groundwork for the development of new intervention strategies to restore iron homeostasis in aging systems.

CHAPTER 2

Deficiency of the RNA-binding Protein Cth2 Extends Yeast Replicative Lifespan by Alleviating its Repressive Effects on Mitochondrial Function

2.1. Abstract

Iron dyshomeostasis contributes to aging, but little information is available about the molecular mechanisms. Here, we provide evidence that, in *Saccharomyces cerevisiae*, aging is associated with altered expression of genes involved in iron homeostasis. We further demonstrate that defects in the conserved mRNA-binding protein Cth2, which controls stability and translation of mRNAs encoding iron-containing proteins, increase lifespan by alleviating its repressive effects on mitochondrial function. Mutation of the conserved cysteine residue in Cth2 that inhibits its RNA-binding activity is sufficient to confer longevity, whereas Cth2 gain-of-function shortens replicative lifespan. Consistent with its function in RNA degradation, we demonstrate that Cth2 deficiency relieves Cth2-mediated post-transcriptional repression of nuclear-encoded components of the electron transport chain. Our findings uncover a major role of the RNA-binding protein Cth2 in the regulation of lifespan and suggest that modulation of iron starvation signaling can serve as a target for potential aging interventions.

2.2. Introduction

Iron (Fe) is an essential trace element, which serves as a cofactor for enzymes involved in multiple metabolic pathways, including synthesis of DNA, ribosome biogenesis, lipid metabolism, and mitochondrial oxidative phosphorylation. Dysregulation

of Fe homeostasis has been implicated in the development of many human age-related diseases including diabetes [29], inflammatory diseases [30], and neurodegeneration [31-34], but little is known about the molecular details of how Fe homeostasis affects aging.

In eukaryotes, Fe utilization and storage are tightly controlled. Yeast *S. cerevisiae* contains two partially redundant transcription factors, Aft1 and Aft2, which activate the expression of genes known as Fe regulon that facilitate mobilization of intracellular Fe stores and its extracellular uptake in response to Fe deficiency [10, 35]. In addition, Aft1 and Aft2 activate the expression of the RNA-binding protein Cth2. This protein contains two tandem zinc fingers (TZFs) that are required for binding AU-rich elements (AREs) present in the 3' untranslated region (UTR) of target mRNAs [12, 36]. When Fe becomes scarce, Cth2 binds mRNAs that encode proteins involved in non-essential Fe-demanding pathways, including mitochondrial oxidative phosphorylation and TCA cycle, and promotes their degradation to prioritize Fe utilization to indispensable processes such as DNA synthesis and repair [11, 12, 37, 38]. Disruption of the TZF RNA-binding domain or mutations of conserved cysteine (Cys) residues within the TZFs to arginine (Arg) prevent binding and decay of Cth2 target mRNAs [12, 39]. More recently, Cth2 has been shown to directly inhibit the translation of several mRNA targets, in addition to its function in mRNA degradation [37, 40]. However, the mechanisms of translational repression by Cth2 remain unknown.

Previous studies have documented dysregulation of Fe homeostasis and activation of the Fe regulon during the aging process. In yeast, impaired Fe/S cluster (ISC) synthesis has been shown to cause age-associated genomic instability [41, 42]. Loss of vacuolar

acidification is an early event during aging that has been linked to increased activity of the Fe regulon and mitochondrial dysfunction [43]. Consistent with these observations, deficiency of the vacuolar ATPase (V-ATPase), which is required for maintaining vacuolar acidity, shortens lifespan [44-46]. In addition, a genetic screen has previously demonstrated that deletion of *CTH2*, which encodes for the Cth2 protein involved in post-transcriptional regulation of Fe homeostasis, as well as its close homolog *CTH1*, extends lifespan in yeast [13].

While previous reports have shown that dysregulation of Fe homeostasis contributes to aging, the underlying molecular mechanisms are still not completely understood. In this study, we investigated how Fe homeostasis influences the aging process by performing unbiased analyses of the yeast deletion mutants lacking genes involved in Fe import and utilization. Here, we show that aging in yeast is associated with an up-regulation of Fe regulon genes whereas deletion of several members of the Fe regulon leads to increased longevity. We also show that constitutive activation of the Aft1 transcription factor shortens lifespan in *S. cerevisiae*. These findings demonstrate that expression of several Fe regulon genes is limiting lifespan in yeast. Finally, we reveal that deficiency of the RNA-binding protein Cth2 is sufficient to prevent the negative effect of Aft1 on lifespan by alleviating its repressive effects on its targets. Together, these findings uncover an important role of the RNA-binding protein Cth2 in the regulation of lifespan and suggest that modulation of Fe homeostasis may serve as an attractive strategy to delay aging and prevent the development of age-associated diseases in humans.

2.3. Results

Modulation of Fe metabolism impacts yeast replicative lifespan and cell fitness.

To understand the impact of Fe homeostasis on cellular aging, we performed unbiased analysis of the effect of deleting genes involved in Fe import and utilization on lifespan in yeast *S. cerevisiae*. To this end, we analyzed replicative lifespan (RLS) of yeast strains lacking an Fe-responsive transcription factor (*AFT1*), as well as genes involved in cellular Fe uptake (*FET3*, *FIT2*), vacuolar Fe storage and mobilization (*CCCI*, *FTH1*, *VMA21*), mitochondrial Fe import (*MRS3*), Fe/S cluster (ISC) synthesis and distribution (*ISU1*, *GRX3*), recycling of heme iron (*HMX1*), and remodeling of cellular Fe metabolism (*CTH1*, *CTH2*) (Figure 1A). Although most of the analyzed gene deletions involved in Fe homeostasis either did not significantly change lifespan or led to a shortened replicative lifespan, we found that deletion of *FET3*, *FIT2*, *HMX1*, *CTH1*, and *CTH2* genes significantly extended lifespan ($p < 0.05$; Figure 1B, Table 1). One of the longest-lived gene deletions, i.e., *CTH2* encoding an RNA-binding protein involved in Fe starvation response, extended lifespan by 51.1% ($p < 0.0001$; Figure 1B, Table 1). We next investigated how perturbations of Fe homeostasis impact cell fitness by analyzing the growth of the gene deletion mutants in the presence of different levels of Fe²⁺ in the media (Figure 2A). We observed that the *aft1*Δ mutant has delayed growth on YPD medium.

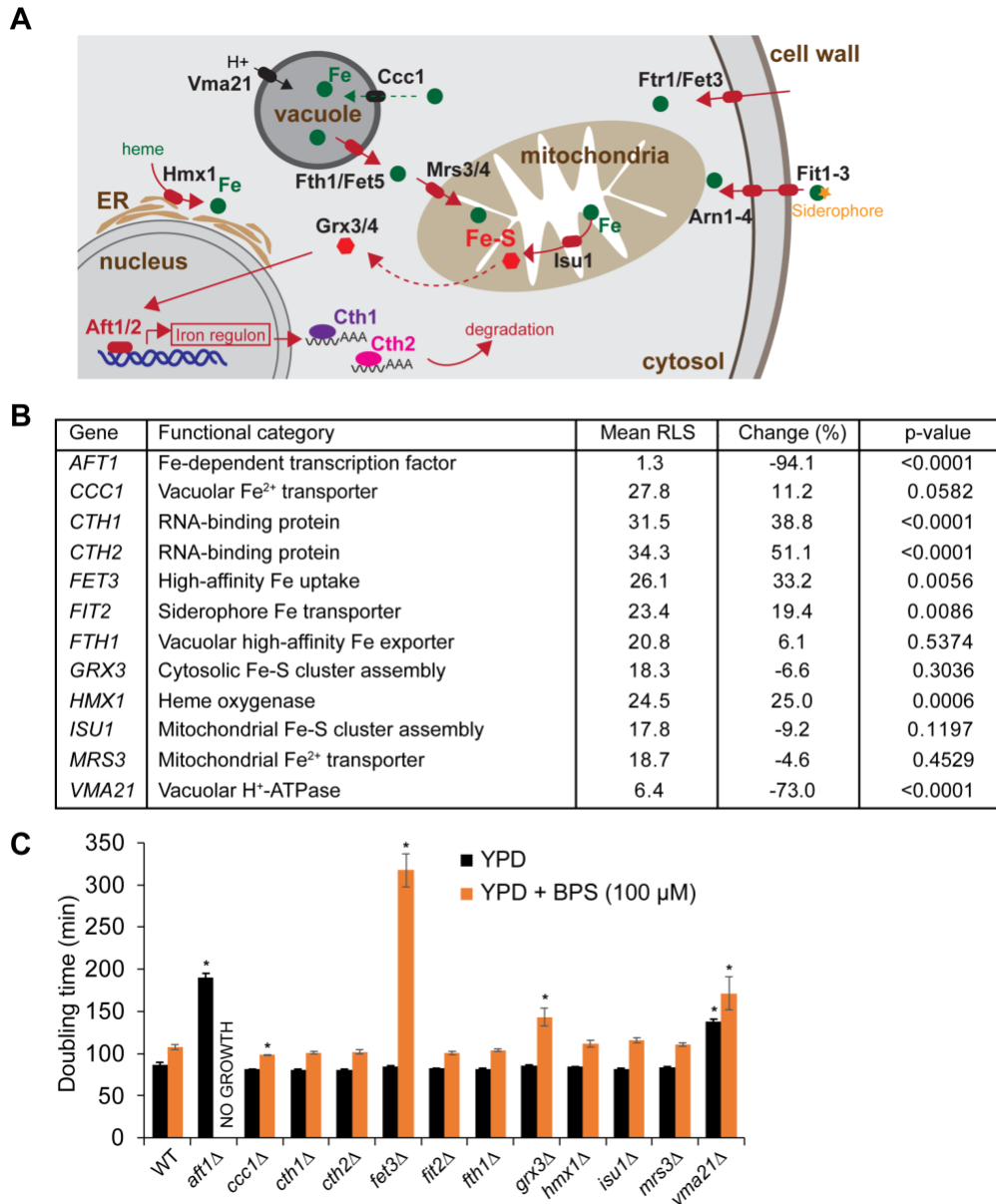


Figure 1. Deletion of genes involved in Fe homeostasis differentially affects lifespan and cell fitness.

(A) Scheme of the Fe regulon in *S. cerevisiae*. Deficiency of the ISC production leads to nuclear localization of the Aft1 transcription factor, which activates expression of the Fe regulon genes involved in Fe assimilation. (B) Replicative lifespan of yeast mutants lacking genes involved in regulation of Fe homeostasis. Pooled data from three biological replicates are shown. (C) Doubling time in the absence or presence of 100 μM Fe²⁺ chelator BPS. Doubling time was calculated using the Yeast Outgrowth Data Analyzer (YODA) software. Error bars represent SEM of three biological replicates, each containing three technical replicates. * $p < 0.05$, compared to wild-type cells, Student's t test.

However, the cell fitness improved when the medium was supplemented with Fe in the form of ferrous ammonium sulfate (FAS). Consistent with prior reports, the growth of *aft1Δ*, *fet3Δ*, and *vma21Δ* cells was impaired on YPG medium containing 3% glycerol (which requires mitochondrial respiration to be utilized), indicating that these mutants are respiratory insufficient [47]) (Figure 2B). However, supplementing YPG with FAS rescued the growth of *vma21Δ* cells, but not *aft1Δ* cells and only partially *fet3Δ* cells. In addition, Fe deficiency significantly delayed the growth rates of the *aft1Δ*, *fet3Δ*, *grx3Δ* and *vma21Δ* mutants ($p < 0.05$) in the presence of Fe^{2+} chelator bathophenanthrolinedisulfonic acid (BPS) [48] (Figure 1C). Together, these data suggest that the deletion of genes involved in different aspects of Fe homeostasis may differentially affect lifespan and cellular fitness.

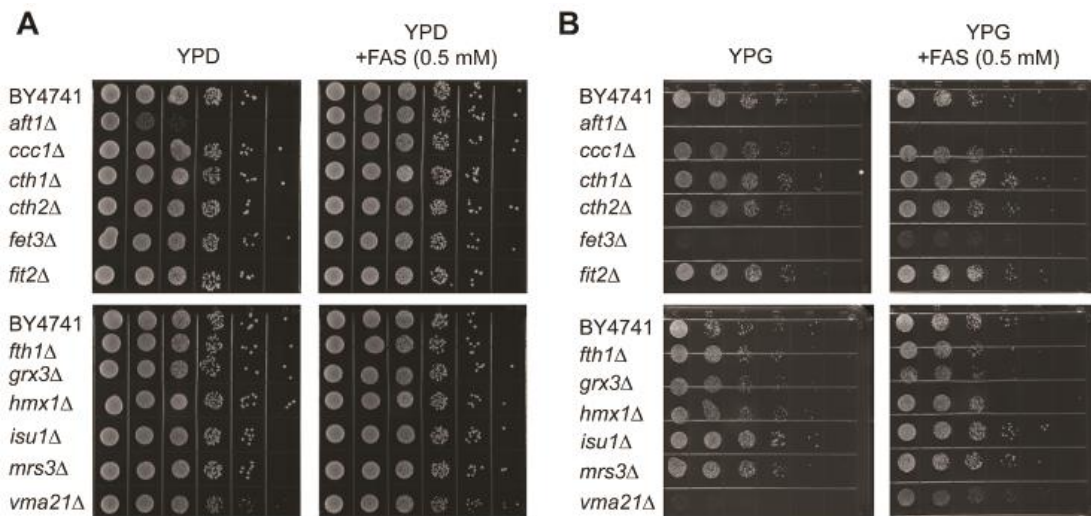


Figure 2. Deletion of genes involved in Fe metabolism differentially affects cell fitness.

(A) Growth of the gene deletion mutants on rich YPD media in the absence and presence of 0.5 mM ferrous ammonium sulfate (FAS). (B) Growth of the mutants on non-fermentable YPG media containing 3% glycerol as a carbon source in the absence and presence of 0.5 mM ferrous ammonium sulfate (FAS). $10\times$ serial dilutions of logarithmically growing cells were spotted and incubated for 48 h at 30 °C.

Old cells demonstrate a global decrease in mRNA translation, but an up-regulation of genes involved in Fe import into the cell.

Previous studies have shown that protein synthesis is globally decreased in yeast during replicative aging [49]. To determine whether overall inhibition of translation during aging leads to a decrease in expression of Fe-related proteins, we examined global protein synthesis levels in young and replicatively aged yeast using ribosome profiling (Ribo-Seq). For this, we isolated replicatively aged cells using the Mother Enrichment Program (MEP) [50, 51] combined with the biotin affinity purification step [52]. We isolated yeast cells that were cultured in the presence of estradiol for 2 h (YNG) and 30 h (OLD) and had undergone on average 2 and 15 cell divisions, respectively (Figure 3A). Following the enrichment of replicatively aged cells, mRNA expression and protein translation profiles were assessed in young and aged cells by RNA-Seq and Ribo-Seq approaches. To account for differences in overall translational changes with aging, we spiked Ribo-Seq samples with 1% worm lysate at the beginning of the library preparation. The addition of the spike-in control from an evolutionarily distant organism allowed us to normalize the samples based on overall translation levels. By comparing the ratio of reads in each of the samples to the number of reads that align to the worm genome, we found that overall levels of protein translation were significantly decreased in replicatively aged cells compared to young cells (Figure 3B).

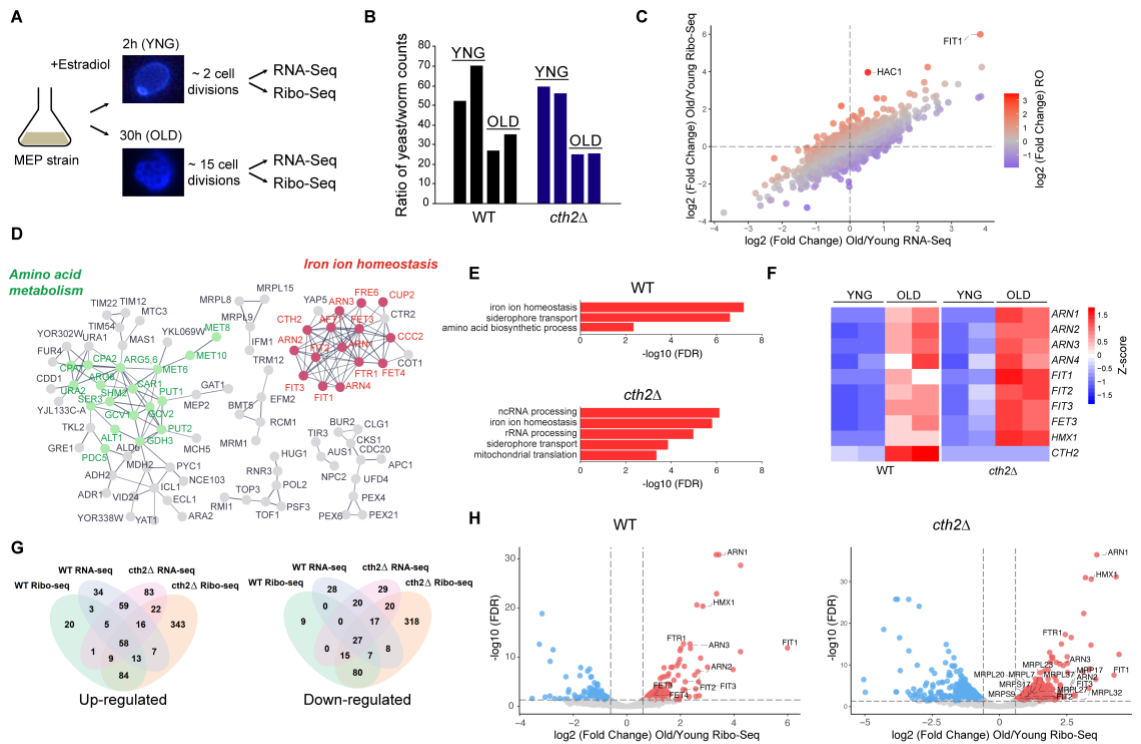


Figure 3. Aging leads to a global inhibition of translation, but an up-regulation of genes involved in Fe homeostasis.

(A) RNA-Seq and Ribo-Seq analyses in young (YNG) and replicatively aged (OLD) cells isolated using the Mother Enrichment Program. (B) Spike-in enables direct comparison of footprints between Ribo-Seq samples. For each sample, two biological replicates were analyzed. (C) Comparison of transcriptional (RNA-Seq) and translational (Ribo-Seq) changes during aging. Genes whose ribosome occupancy (RO) is increased (red) or decreased (blue) with aging are highlighted. (D) Genes significantly up-regulated during aging ($\text{FDR} < 0.05$) identified by Ribo-Seq were visualized using STRING (evidence view, high confidence). Genes without network partners were omitted. (E) Gene ontology analysis of the Ribo-Seq data indicates activation of pathways involved in Fe uptake during aging. (F) *CTH2* expression is upregulated during aging. Heatmap shows scaled expression values (normalized \log_2 Ribo-Seq read counts) of the Fe regulon genes, including *ARN1*, *ARN2*, *ARN3*, *ARN4*, *FIT1*, *FIT2*, *FIT3*, *FET3*, *HMX1*, and *CTH2*, in young (YNG) and replicatively aged (OLD) wild-type and *cth2Δ* cells. (G) Venn diagrams show common significantly changed transcripts at the level of transcription (RNA-seq) and translation (Ribo-seq) in wild-type and *cth2Δ* cells ($\text{FDR} < 0.05$). (H) Cth2 is a negative regulator of mitochondrial translation. Volcano plot shows differentially translated genes ($\text{FDR} < 0.05$, Log_2 fold change > 0.6) in wild-type and *cth2Δ* cells.

We next compared temporal changes in mRNA expression and protein translation in replicatively aged cells using the RNA-seq and Ribo-seq data. Most of the age-

dependent changes detected by Ribo-seq correlated with the changes in the transcriptome (Figure 3C) suggesting that most of the changes of gene expression during aging occur at the level of transcription. Despite the overall decrease in translation, our analysis revealed an up-regulation of genes involved in Fe ion homeostasis, siderophore transport, and amino acid biosynthesis with aging (Figure 3D and 3E). Interestingly, most of the up-regulated genes involved in Fe ion homeostasis are key components of the Fe regulon, a group of genes regulated by the Aft1 transcription factor [53]. Together, our data indicate that aging is associated with a global inhibition of translation, but an up-regulation of genes involved in Fe import into the cell.

Ribo-Seq analyses reveal mitochondrial translation as a post-transcriptional target of Cth2.

Ribo-Seq analyses of replicatively aged cells showed that expression of the RNA-binding protein Cth2, which is involved in post-transcriptional repression of genes encoding for non-essential Fe-containing proteins, increases during aging (Figure 3F). The fact that levels of Cth2 are increased with aging, whereas the deletion of *CTH2* extends lifespan suggests that Cth2 might be a negative regulator of longevity. To further understand the biological relevance of Cth2 during aging, we used Ribo-Seq to perform genome-wide analysis of translation in young and old *cth2Δ* mutant cells. Our analysis revealed that most changes observed in wild-type cells with aging were also detected in the *cth2Δ* mutant (Figure 3G). Ribo-Seq identified 552 up-regulated genes and 492 down-regulated genes in the *cth2Δ* mutant with aging (FDR<0.05), of which 164 were commonly up-regulated with aging and 129 genes were commonly down-regulated with aging in both

wild-type and the *cth2Δ* mutant. To distinguish between transcriptional and translational responses, we compared changes in gene expression in replicatively aged *cth2Δ* cells identified by the RNA-Seq and Ribo-Seq approaches. Although most of the changes in gene expression during aging were driven by changes in mRNA abundance, we identified 343 genes that were specifically up-regulated in the *cth2Δ* mutant at the level of translation (Figure 3G).

Cth2 is an mRNA-binding protein that acts as a posttranscriptional regulator by affecting stability and translation of mRNAs containing the 5'-UAUUUAUU-3' and 5'-UUAUUUAU-3' AU-rich elements (AREs) in their 3' untranslated (UTR) regions [12, 37]. In response to Fe deprivation, Cth2 binds mRNAs encoding Fe-containing proteins, leading to their degradation. In addition to known Cth2 targets, our data revealed that Cth2 is limiting the expression of genes involved in mitochondrial translation and genes encoding for mitochondrial ribosomal proteins. Among the genes translationally up-regulated in the *cth2Δ* mutant, we identified 24 genes involved in mitochondrial translation, including 11 ribosomal proteins of the small subunit and 12 ribosomal proteins of the large subunit (Figure 3H and Figure 4). However, most of these Cth2-dependent genes do not possess AREs in their 3'-UTR sequences suggesting that they might be coordinately regulated by Cth2, but not directly. Further computational analyses of genes whose ribosome occupancy was significantly changed in *cth2Δ* cells with aging revealed the presence of Puf3 binding sequences within 3'-UTRs (Table S2). Puf3 functions as an mRNA-binding protein that binds mRNAs coding for mitochondrial ribosomal proteins

and inhibits their translation strongly suggesting Puf3 as a potential regulator by which Cth2 mediates changes in mitochondrial translation [54].

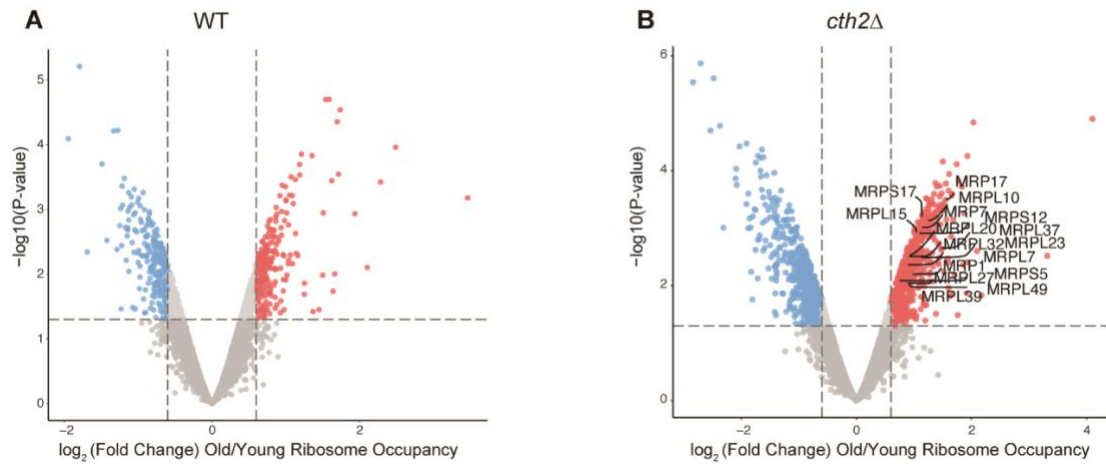


Figure 4. Comparison of ribosome occupancy changes during aging.

Log₂ fold changes in ribosome occupancy (RO) during aging in wild-type (A) and *cth2Δ* (B) cells were calculated with EdgeR. Genes involved in mitochondrial translation whose Log₂ fold change in RO is greater than 0.6 ($p < 0.05$) are shown.

Together, the evidence that Cth2 affects mitochondrial translation and the known role of Cth2 in limiting Fe for non-essential processes and down-regulating respiration, suggest Cth2 as a negative regulator of mitochondrial function during aging.

Constitutive activation of the Fe regulon shortens lifespan in *S. cerevisiae*.

We hypothesized that increased activity of Aft1 transcription factor in old cells leads to increased levels of Cth2, which might negatively regulate longevity by repressing mitochondrial function. To test this hypothesis, we first asked whether constitutive

activation of the Fe regulon in young cells is sufficient to shorten lifespan in *S. cerevisiae*.

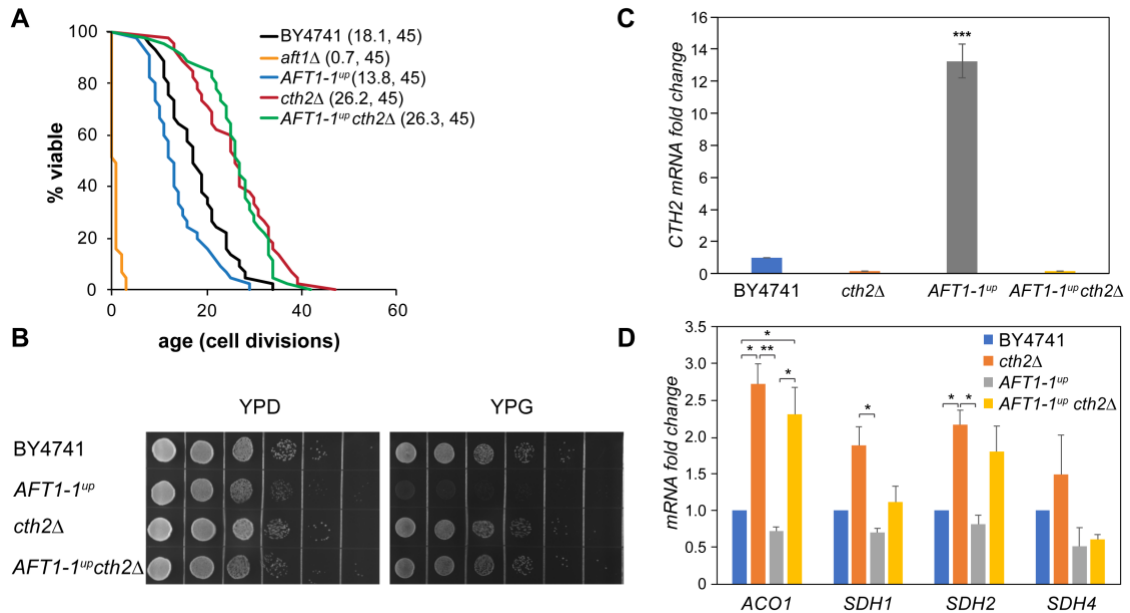


Figure 5. Constitutive activation of the Aft1 negatively regulates yeast lifespan.

(A) Shortened lifespan in cells expressing *AFT1-1^{up}* allele can be rescued by the deletion of *CTH2*. Mean lifespans and the number of cells assayed are shown in parentheses. Pooled data from three biological replicates are shown. (B) Constitutive activation of the Aft1 transcription factor using *AFT1-1^{up}* allele leads to inability to grow on glycerol containing medium (YPG), whereas deletion of *CTH2* is able to rescue this growth defect. 10× serial dilutions of logarithmically growing cells were spotted on agar plates with YPD (glucose) or YPG (glycerol) media. (C) Expression of *AFT1-1^{up}* induces expression of Cth2. Relative mRNA levels of *CTH2* in exponentially growing cells were determined by RT-qPCR. Results are represented as means ± SEM of three biological replicates, *** $p < 0.001$ compared to wild-type control (one-way ANOVA). (D) Deletion of *CTH2* alleviates its repressive effects on its targets. Relative mRNA levels of Cth2 targets in exponentially growing cells were determined by RT-qPCR. Results are represented as means ± SEM of three biological replicates, * $p < 0.05$, ** $p < 0.01$ compared to wild-type control (one-way ANOVA).

For this, we generated a yeast strain carrying a genome-integrated copy of the *AFT1-1^{up}* allele [55] and analyzed its replicative lifespan. This strain contains a mutation in the Aft1 protein that leads to its nuclear accumulation and constitutive expression of the Fe regulon genes, irrespective of Fe availability. We found that constitutive activation of

the Fe regulon by *AFT1-I^{up}* allele significantly decreased the replicative lifespan of yeast cells ($p < 0.01$; Figure 5A, Table 1). To ascertain whether the up-regulation of *CTH2* by the *AFT1-I^{up}* allele contributes to shortened lifespan in *AFT1-I^{up}* expressing cells, we combined the constitutively active *AFT1-I^{up}* allele with the *cth2Δ* deletion. Importantly, deletion of *CTH2* was able to rescue the short lifespan of *AFT1-I^{up}* allele expressing cells (Figure 5A) suggesting a negative effect of the increased Cth2 expression on lifespan.

Because many of the Cth2 targets include mRNAs encoding for mitochondrial proteins and components of the mitochondrial electron transport chain, one would expect that constitutive activation of Aft1 transcription factor would increase *CTH2* expression and inhibit mitochondrial function leading to the inability to grow on non-fermentable carbon sources that require respiration. The growth of the *AFT1-I^{up}* allele expressing cells was significantly impaired on the non-fermentable medium containing glycerol as the only carbon source [56] (Figure 5B). Moreover, deletion of *CTH2* was able to rescue the growth of the *AFT1-I^{up}* expressing cells on glycerol-containing medium. Finally, in agreement with Cth2 function in mRNA degradation, our data show that constitutive activation of the Aft1 transcription factor leads to increased expression of Cth2 (Figure 5C) and Cth2-dependent decrease in levels of mRNA coding for nuclear-encoded components of the electron transport chain and the TCA cycle (Figure 5D). These findings suggest that age-dependent activation of the Aft1 transcription factor could contribute to aging in *S. cerevisiae* and lead to impaired mitochondrial function by increasing expression of the Cth2 post-transcriptional regulator.

Blocking mRNA-binding activity of Cth2 extends lifespan whereas increasing levels of Cth2 is sufficient to shorten lifespan in yeast.

To investigate the underlying mechanisms by which Aft1-dependent activation of *CTH2* expression negatively regulates longevity, we asked whether blocking mRNA-binding activity of Cth2 is sufficient to extend lifespan. Cth2 contains an RNA-binding motif consisting of two tandem zinc fingers (TZFs), which directly interact with AREs within the 3'-UTR regions of its target mRNAs [11, 12]. Mutations of the conserved Cys residues within the TZF domain of Cth2 have been shown to abolish Cth2 binding of its target mRNAs and their subsequent degradation [12]. To test whether the mRNA-binding function of Cth2 is directly related to its repressive effect on lifespan, we examined if mutation of the conserved Cys residue within the TZF domain to Arg (C190R) is sufficient to extend lifespan (Figure 6A).

We found that the replicative lifespan of the *CTH2-C190R* mutant was increased to a similar extent as the *cth2Δ* mutant (21.4%, $p < 0.01$ compared to wild-type control; Figure 6B, Table 1). These data demonstrate that the integrity of the TZFs and RNA-binding function of Cth2 are required for its repressive effects on lifespan.

Recently, phosphorylation of a patch of serine residues within the N-terminal region of Cth2 has been shown to play an important role in its ubiquitin-dependent degradation [57]. When Cth2 degradation is impaired by mutagenesis of the Cth2 serine residues, the levels of Cth2 protein increase leading to impaired growth in Fe-depleted conditions [36, 57]. To

further test how increased levels of Cth2 affect lifespan, we used a Cth2 double serine -

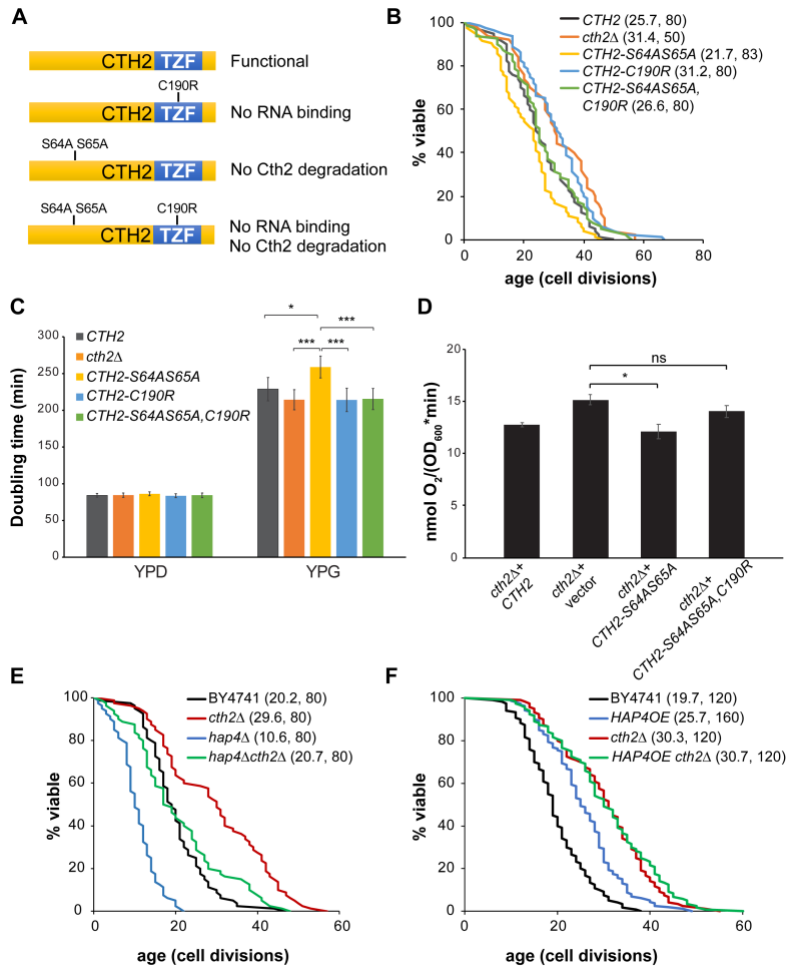


Figure 6. Cth2 is a negative regulator of lifespan and mitochondrial respiration.

(A) Schematic representation of the Cth2 wild-type and mutant proteins used in this study. (B) Mutation of the conserved Cys residue within the TZF domain of Cth2 to Arg (C190R) is sufficient to extend lifespan. Mean lifespans and the number of cells assayed are shown in parentheses. Pooled data from three biological replicates are shown. (C) Doubling times in YPD and the non-fermentable YPG media were calculated using Yeast Outgrowth Data Analysis (YODA) software. Error bars represent SEM of three biological replicates, *** $p < 0.001$, * $p < 0.05$ (two-way ANOVA). (D) Increased expression of Cth2 inhibits mitochondrial respiration. Oxygen consumption was measured in cells grown in YPG medium for 29 h. Error bars represent SEM of three biological replicates, ns: not significant, * $p < 0.05$ (two-way ANOVA). (E) Extended lifespan in *cth2Δ* is dependent on the Hap4 transcription factor. (F) Hap4 overexpression (*HAP4OE*) and *cth2Δ* do not have an additive effect on lifespan. Mean lifespans and the number of cells assayed are shown in parentheses. Pooled data from three biological replicates are shown.

mutant (*CTH2-S64A,S65A*) allele either alone or in combination with the TZF mutant (*CTH2-C190R*) (Figure 6A).

Our data demonstrate that the *CTH2-S64A,S65A* (gain-of-function) mutant allele shortens lifespan (15.6%, $p < 0.05$ compared to wild-type control; Figure 6B, Table 1). Conversely, combining the Cth2 double serine mutant (*CTH2-S64A,S65A*) with the TZF loss-of-function mutation (*CTH2-C190R*) abolished its negative effect on lifespan. Together, these data suggest that the non-degradable form of Cth2 protein has a deleterious effect on lifespan.

Cth2 is a negative regulator of mitochondrial function.

Previous studies revealed a correlation between oxygen consumption and increased levels of mitochondrial respiration with lifespan extension in yeast [58-60]. Because targets of Cth2 include components of the mitochondrial electron transport chain and TCA cycle, we hypothesized that increased levels of Cth2 would inhibit mitochondrial function leading to decreased respiration. To test this, we analyzed the growth of cells expressing the non-degradable double serine Cth2 mutant (*CTH2-S64A,S65A*), the TZF domain mutant (*CTH2-C190R*), and the *CTH2-S64A,S65A,C190R* mutant in YPG medium containing glycerol as a carbon source that requires respiration (Figure 6C). We observed that the population doubling time of the cells expressing a non-degradable form of Cth2 (*CTH2-S64A,S65A*) was significantly increased ($p < 0.01$) in YPG medium compared to *cth2Δ* and *CTH2-C190R* mutant cells. Moreover, introducing the C190R mutation that blocks RNA-binding activity of Cth2 completely prevented this effect. To further assess that this effect is due to decreased respiration, we measured the levels of oxygen consumption in YPG

medium in the *cth2Δ* mutant as well as in cells expressing *CTH2-S64A,S65A* and *CTH2-S64A,S65A,C190R* mutations (Figure 6D). We found that the strain expressing the *CTH2-S64A,S65A* mutation has significantly decreased ($p < 0.05$) oxygen consumption, whereas mutation in the TZF domain (*CTH2-S64A,S65A,C190R*) abolished this effect.

Overexpression of the Hap4 transcription factor, which controls the expression of many genes encoding components of the mitochondrial electron transport chain, has been shown to extend *S. cerevisiae* lifespan by increasing respiration [59]. Given that Cth2 affects the expression of the respiratory genes at the post-transcriptional level, we asked whether increased lifespan in the *cth2Δ* mutant is dependent on the Hap4 transcription factor. Consistent with this possibility, deletion of *HAP4* significantly decreased the lifespan in the *cth2Δ* background (30.1%, $p < 0.001$; Figure 6E, Table 1). To further validate that Cth2 deficiency extends lifespan by affecting mitochondrial respiration, we performed an epistasis experiment combining *cth2Δ* with Hap4 overexpression (*HAP4OE*). As expected, combining *cth2Δ* with *HAP4OE* had no additive effect on lifespan (Figure 6F, Table 1). Taken together, our data suggest that Cth2 is a negative regulator of lifespan, which accumulates with aging and down-regulates its downstream targets leading to Cth2-dependent repression of mitochondrial respiration.

2.4. Discussion

Dysregulation of Fe homeostasis has been implicated in the development of many human age-related diseases such as type 2 diabetes, cancer, neurodegeneration, and cardiovascular disease. However, how Fe homeostasis contributes to organismal aging remains unclear. Previous studies have also shown that aging in model organisms is

associated with a decline of mitochondrial function and activation of genes involved in Fe homeostasis, but the link between these processes and aging is not completely understood [41, 61]. Here, we performed an unbiased screen to investigate how deletion of individual genes involved in Fe import and utilization affects lifespan using yeast *S. cerevisiae* as a model. Although the majority of the tested deletion mutants did not significantly change lifespan, we found that deletion of several members of the Fe regulon, including *FET3*, *FIT2*, *HMX1*, *CTH1* and *CTH2*, led to increased longevity (Figure 1). These data, together with the observation that activity of the Fe regulon is increased during aging, suggest a model that increased expression of the Aft1 targets might limit replicative lifespan in yeast. In support of this model, our data show that expression of the constitutively active Aft1 mutant (*AFT1-I^{up}*) allele, which activates Fe regulon genes irrespective of the Fe availability, leads to shortened lifespan.

One of the longest-lived mutants we analyzed lacks *CTH2*, a gene encoding an RNA-binding protein that post-transcriptionally regulates Fe-related proteins during Fe deficiency [13]. *CTH2* is also one of the major transcriptional targets that are activated by the Aft1 transcription factor, which showed a robust increase during aging. Here, we propose that Cth2-dependent repression of its targets mediates the negative effects of Aft1 on lifespan leading to repression of mitochondrial function. In agreement with this hypothesis, deletion of *CTH2* in cells expressing *AFT1-I^{up}* allele was able to abolish the negative effect of *AFT1-I^{up}* on lifespan. Since Cth2 targets include many mitochondrial genes involved in TCA cycle and respiration [12, 37], one would expect that increased expression of Cth2 would inhibit mitochondrial function leading to decreased respiration.

Indeed, our data demonstrate that Cth2 negatively regulates respiration. In addition, we show that the *AFT1-1^{up}* allele expressing cells were unable to grow on non-fermentable carbon sources, but deletion of *CTH2* was sufficient to alleviate the negative effects of Aft1 expression on respiration.

Due to its involvement in the regulation of respiration and other Fe-dependent pathways, derepression of Cth2 targets in the *cth2Δ* mutant may explain the effect of Cth2 loss on lifespan. Mutation of the conserved Cys residue within the TZF domain of Cth2 that inhibits its mRNA-binding activity was sufficient to confer longevity, whereas Cth2 gain-of-function shortened replicative lifespan. These data suggest that deletion of *CTH2* extends lifespan by directly alleviating mRNA-binding and its repressive effects on its targets. Specifically, we show that that expression of constitutively active *AFT1-1^{up}* allele leads to increased expression of Cth2 and Cth2-dependent repression of the components of the electron transport chain and the TCA cycle leading to repression of mitochondrial function. Consistent with the repressive effect of Cth2 on respiration, deletion of *GRR1* gene in yeast has been shown to prevent the growth of cells on media with non-fermentable carbon sources [57]. Grr1 is the protein that recognizes phosphorylated Cth2 and facilitates its proteasomal degradation [57, 62]. Therefore, elevated Cth2 protein levels in the *grr1Δ* mutant might inhibit the growth of cells on non-fermentable carbon sources through Cth2-mediated degradation of its targets. The role of Cth2 as a negative regulator of mitochondrial function is further supported by the fact that deletion of *CTH2* in *grr1Δ* prevented the negative effect of Cth2 on growth in YPEG medium [57]. Moreover, we demonstrate that overexpression of the Hap4 transcription factor, which has been shown to

extend lifespan by increasing respiration [59, 63], had no additive effect on lifespan with the deletion of *CTH2*. Together, these data suggest that Cth2 is a negative regulator of mitochondrial function and longevity.

We also identified mitochondrial translation as a post-transcriptional target of Cth2. Although many of the prior studies investigated changes in gene expression during aging at the transcriptional level across multiple species, the role of post-transcriptional regulation in aging is much less understood. By applying a combination of the RNA-Seq and Ribo-Seq approaches, we identified genes that are specifically regulated by Cth2 at the post-transcriptional level during aging. Although many of the mitochondrial ribosomal proteins were activated in the *cth2* Δ mutant with aging, most of them do not contain putative ARE sequences in their 3'-UTR. One possibility is that these proteins are regulated by a common transcription or translation factor that is directly regulated by Cth2. Further studies are required to investigate the mechanism of how Cth2 regulates mitochondrial translation. Together, Cth2-dependent inhibition of mitochondrial respiration and repression of mitochondrial translation may contribute to mitochondrial dysfunction during aging.

Limitations of the Study

Together, our data demonstrate that dysregulation of Fe homeostasis negatively regulates longevity through the increased activity of the Aft1 transcription factor and the Cth2 mRNA-binding protein function (Figure 7). However, several important questions

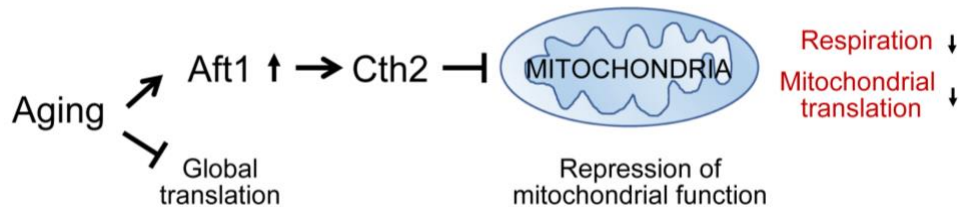


Figure 7. Model showing the role of Cth2 in age-related repression of mitochondrial function.

During aging, increased activity of the Aft1 transcription factor leads to increased expression of Cth2, which targets mRNAs involved in respiration and mitochondrial translation, leading to repression of mitochondrial function.

remain. First, the mechanism by which the activity of Aft1 is increased. Whether the activation of the Fe regulon genes is because old cells experience Fe deficiency or it is a result of aberrant expression of Aft1 transcription factor, even in the presence of sufficient Fe in the cell, requires further investigation. Second, the relationship between Fe homeostasis and other aging pathways is poorly understood. Third, it will be important to determine whether the role of Cth2 in regulating longevity is evolutionarily conserved. Notably, deficiency of the orthologous protein in *Caenorhabditis elegans*, *pos-1*, significantly extends the animal's lifespan [64, 65]. Given that the mammalian homolog of Cth2, called tristetruprolin (TTP), also post-transcriptionally modulates the expression of Fe metabolism-related genes including transferrin receptor 1 and genes involved in mitochondrial electron transport chain [18, 66], our study raises a possibility that modulation of Fe starvation signaling can serve as a target for potential aging interventions in humans.

2.5. Methods

Experimental model

Single gene deletion mutants were derived from the Yeast Knockout Collection. To construct double knockout strains, one-step PCR-mediated gene disruption was performed using standard techniques. Cells were grown at 30°C in standard YPD medium (1.0% yeast extract, 2.0% peptone, and 2.0% glucose) unless otherwise stated. To purify aged cells for RNA-Seq and Ribo-Seq analyses, we used *MEP* and *MEP cth2Δ* strains expressing the yeast Mother Enrichment Program (MEP) [51, 67]. *MEP* and *MEP cth2Δ* cells were grown under nourseothricin (NAT) (100 μg/mL) and Hygromycin B (300 μg/mL) selection. To create yeast strains expressing *CTH2*, *CTH2-C190R*, *CTH2-S64A,S65A*, and *CTH2-S64A,S65A ,C190R*, *AFT1-1^{up}*, and *ADH1pr-HAP4*, their corresponding sequences were amplified by PCR and integrated into the BY4741 genome.

Method details

One-step PCR-mediated gene disruption was performed using standard techniques. All genotypes were verified using single colony screening with polymerase chain reaction (PCR).

To create BY4741 yeast strains expressing *CTH2*, *CTH2-C190R*, *CTH2-S64A,S65A*, and *CTH2-S64A,S65A ,C190R*, their corresponding ORFs were amplified from plasmids pSP414, pSP429, pSP853, and pSP898, respectively [57]. PCR amplified *CTH2* and *CTH2* with mutations were then cloned into pDZ415 [68] by using NotI and Sall restriction sites upstream of loxP-KanMX-loxP. Then *CTH2* and *CTH2* with mutations along with loxP-KanMX-loxP were amplified using the primers flanked on the 5' side by sequence

homologous to *CTH2* ORF and the 3' side by sequence homologous to *CTH2* 3'-UTR for genomic integration. After the integrations were confirmed with colony PCR, cells were transformed with 0.2 μ g pSH47 (Cre recombinase) for removal of KanMX marker [69] and the transformants were selected on SC medium lacking uracil. After the transformation of the pSH47, cells were incubated overnight in YP medium supplemented with 3% galactose for the induction of Cre recombinase. The culture was subsequently diluted in 10-fold dilutions and plated out on YPD medium and incubated at 30 °C for 30 h. The resulting colonies were replica-plated on YPD and YPD with 200 μ g/ml G418 for the selection of colonies that lost the KanMX marker and verified by colony PCR.

To generate the *AFT1-I^{up}* strain, *AFT1-I^{up}* sequence was amplified using pAFT1-1UP [70] and integrated into the BY4741 genome using the same procedure that was used to create *CTH2* mutant yeast strains above.

To create the *HAP4OE* strain expressing an *ADHI* promoter driven *HAP4* (*ADHIpr-HAP4*), a 705 bp fragment of the *ADHI* promoter was cloned into pRS306 using NotI and XhoI restriction sites. The fragment containing URA3 along with the *ADHI* promoter was then PCR amplified using the oPP274 and oPP275 oligonucleotides (homologous to the 3' end of the *HAP4* promoter and 5' end of the *HAP4* ORF, respectively) and used for genomic integration.

Spot Assays

The growth of strains on YPD and YPG media containing 3% glycerol as carbon source was determined using spot assays. Cells were initially grown in liquid culture until OD₆₀₀ = 0.6, and 10 \times serial dilutions for each strain were spotted on YPD or YPG agar plates in

the absence and presence of 0.5 mM ferrous ammonium sulfate. The plates were incubated at 30°C, and images were taken 48 h after plating.

Replicative Lifespan

Lifespan assays were carried out as described [71]. Cells were grown on freshly prepared YPD plates at 30°C. Cells were monitored for cell divisions until cells stopped dividing and subsequent daughter cells were removed using a micromanipulator. Replicative lifespan was calculated as the number of times each mother cell divided before it underwent senescence. The lifespan assays were repeated at least three times and the data from three biological replicates were pooled. The number of cells assayed and statistics of the lifespan experiments are shown in Table 1.

Growth Rate Analyses

Yeast growth rates were analyzed using the Epoch 2 Microplate Spectrophotometer (BioTek) and the doubling time interval was calculated using the yeast outgrowth data analyzer (YODA) as described [72, 73]. Results are represented as means \pm SEM of at least three independent experiments. Statistical significance of the data was determined by calculating p values using Student's t test unless otherwise noted.

Isolation of young and old yeast cells

Single colonies were inoculated in 5 mL YPD containing NAT and Hygromycin B and grown overnight at 30°C. The next day cells were diluted to $OD_{600}=0.2$ into 20 mL of the fresh medium and grown until cells reach log phase. Cells were collected by centrifugation at 1000 x g for 3 min, washed twice in sterile PBS and 3×10^8 cells were used for 30 min biotin labeling (5 mg/mL, EZ-Link Sulfo-NHS-LC-Biotin, Thermo Fisher). Excess Biotin

was quenched with 0.1 M Glycine and cells were resuspended in sterile PBS before inoculation into fresh YPD medium containing 1 μ M estradiol to initiate the Mother Enrichment Program. The 3×10^8 cells were split between young (2 hrs after induction) and old (30 hrs after induction). For each sample, two biological replicates were prepared. Cells were collected by centrifugation at 1000 x g for 3 min, resuspended in ice cold PBS+BE (1 mg/mL BSA + 2 mM EDTA) and incubated for an hour at +4°C with Dynabeads Biotin Binder (Thermo Fisher). Cells were repeatedly washed with ice-cold sterile PBS while on magnet. Finally, sorted cells were counted and recovered in regular YPD 2% glucose for 30 min at 30°C on shaker before collection, flash frozen in liquid nitrogen and stored at -80°C. For each condition, two cell sortings were combined in order to reach at least 1×10^8 cells necessary to make the RNA-Seq and ribosome profiling libraries.

Ribosome Profiling

Yeast extracts were prepared by cryogrinding the cell paste with BioSpec cryomill. The cell paste was re-suspended in lysis buffer (20mM Tris-HCl pH8, 140mM KCl, 5mM MgCl₂, 0.5mM DTT, 1% Triton X-100, 100 μ g/mL cycloheximide), spun at 20,000xg at 4°C for 5 min and 1 mL of the supernatant was transferred to a new Eppendorf tube. To normalize raw reads obtained from young and old cells, an equal amount of worm lysate was added to final concentration of 1% to each sample. After homogenization and spike-in normalization, samples were divided into two tubes, for total mRNAs and footprint extraction. The RNA-seq and ribosome profiling libraries were prepared as described [74] and sequenced using the Illumina HiSeq platform. Ribosomal footprint and total mRNAs reads were aligned to the *S. cerevisiae* genome from the Saccharomyces Genome Database

(<https://www.yeastgenome.org/>, release number R64-2-1) and to the *C. elegans* genome (NCBI, WBcel235 assembly, RefSeq GCF_000002985.6) for linear normalization [49, 75]. Sequence alignment was performed using STAR software 2.7.1a, allowing two mismatches per read [76]. Counts were generated with featureCounts from Rsubread 1.22.2 package [77]. Identification of differentially expressed genes was performed using generalized linear model of the EdgeR package, FDR<0.05 [78].

Ribosome occupancy analysis

To estimate translational efficiency changes in old cells, we analyzed ribosomal occupancy (RO), which represents a ratio between ribosomal footprints and mRNA abundance and, thus, allows us to identify actively translated transcripts. To calculate RO, first, genes with low counts (less than 10 counts) were filtered out from RNA-Seq and Ribo-Seq datasets containing raw counts. RNA-Seq and Ribo-Seq data were next RLE normalized (“Relative Log Expression” normalization) using edgeR package [78]. Finally, we calculated RO using the formula: $\log_2(\text{Ribo-seq counts} + 1) - \log_2(\text{RNA-seq counts} + 1)$. Limma package was used to estimate statistical significance of RO data and identify differentially expressed genes (FDR<0.1) [79, 80].

RT-qPCR

Total RNA was isolated by hot acid phenol extraction. RNA was treated with DNaseI, and 1 μg of RNA was used for cDNA synthesis using SuperScript III reverse transcriptase (Thermo Fisher Scientific) with random hexamer primers according to manufacturer’s instructions. mRNA expression was then analyzed by real-time PCR using KAPA SYBR FAST qPCR Master Mix (Kapa Biosystems) and the CFX-96 Touch Real-Time PCR

Detection System (Bio-Rad Laboratories). *ACT1* was used as a reference gene for normalization of mRNA expression between genotypes. Results are represented as means \pm SEM from three independent experiments.

Analysis of oxygen consumption

Oxygen uptake by cells was measured after growing cells in YPG medium for 29 h using a Clark-type oxygen electrode (Oxyview system, Hansatech). The oxygen consumption rate was expressed as nmol O₂ consumed per minute per OD₆₀₀ (nmol O₂/(min X OD₆₀₀)) and was taken as an index of the respiratory ability. Statistical significance of oxygen consumption data was determined using two-way ANOVA.

Quantification and statistical analysis

Statistical analysis was performed using Prism 9.3.1 (GraphPad Software, Inc). Statistical significance of the RT-qPCR data was determined by calculating p values using one-way ANOVA. Error bars represent standard errors of the means (SEM). The information about number of replicates and P values can be found in figure legends. The lifespan assays were repeated at least three times and the data from three biological replicates were pooled. The number of cells assayed and statistics of the lifespan experiments are shown in Table 1. Statistical significance of the lifespan data was determined using the Wilcoxon Rank-Sum test [81]. For RNA-Seq and Ribo-Seq analyses two biological replicates were analyzed per each condition.

CHAPTER 3

Ribosome Profiling Reveals the Role of Yeast RNA-binding Proteins Cth1 and Cth2 in Translational Regulation

3.1. Abstract

Iron serves as a cofactor for enzymes involved in several steps of protein translation, but the control of translation during iron limitation is not understood at the molecular level. Here, we report a genome-wide analysis of protein translation in response to iron deficiency in yeast using ribosome profiling. We show that iron depletion affects global protein synthesis and leads to translational repression of multiple genes involved in iron-related processes. Furthermore, we demonstrate that the RNA-binding proteins Cth1 and Cth2 play a central role in this translational regulation by repressing the activity of the iron-dependent Rli1 ribosome recycling factor and inhibiting mitochondrial translation and heme biosynthesis. Additionally, we found that iron deficiency represses *MRS3* mRNA translation through increased expression of antisense long non-coding RNA. Together, our results reveal complex gene expression and protein synthesis remodeling in response to low iron, demonstrating how this important metal affects protein translation at multiple levels.

3.2. Introduction

Iron (Fe) is an essential trace element that serves as a cofactor for enzymes involved in numerous cellular processes, including protein translation, DNA replication and repair, lipid biosynthesis, and mitochondrial oxidative phosphorylation [82]. Dysregulation of Fe

homeostasis has been implicated in health and disease. In humans, Fe deficiency causes anemia and leads to the decline of immune, neuronal, and muscle functions [83, 84]. On the other hand, Fe overload leads to organ failure, due to Fe toxicity, and the development of several disorders, such as Alzheimer's disease, cancer, and delayed wound healing [85]. Moreover, imbalance in Fe metabolism has been implicated in aging and age-associated organ failure, but the exact mechanisms remain unclear [86]. A better understanding of the mechanisms by which cells adapt to changes in Fe availability is required for the development of targeted therapeutic strategies against diseases associated with the dysregulation of Fe homeostasis.

Yeast *Saccharomyces cerevisiae* has proven to be a useful model for understanding the basic mechanisms of adaptation of eukaryotic cells to Fe depletion. Previous studies in yeast have shown that Fe deficiency leads to significant changes in gene expression [12, 87, 88]. These changes are mediated by the Aft1 and Aft2 transcription factors, which activate the transcription of ~35 genes known as the "Fe regulon". Expression of these genes allows cellular adaptation to low Fe through several mechanisms: (i) increasing Fe uptake into the cell, (ii) mobilizing Fe from vacuolar stores, and (iii) recycling Fe by promoting heme degradation [10, 38, 87]. In addition, cells adapt to Fe deficiency by dropping the utilization of Fe for non-essential metabolic pathways and shifting to Fe-independent metabolism through the increased expression of the mRNA-binding protein Cth2, which is under the control of the Aft1/2 transcription factors. Cth2 recognizes and binds to AU-rich sequences (5'-UAUUUAUU-3' and 5'-UUAUUUAU-3') in the 3' untranslated region (3'UTR) of several mRNAs coding for proteins containing Fe as a

cofactor (including aconitase, succinate dehydrogenase, and components of the mitochondrial electron transport chain) and stimulate their degradation [12]. A paralog of Cth2, named Cth1, is 46% identical to Cth2, recognizes similar consensus sequences, and can repress the expression of a partially overlapping set of target genes [11, 12, 37]. Thus, Cth1 and Cth2 remodel Fe metabolism prioritizing Fe for proteins involved in essential processes such as DNA replication and repair [89].

While transcriptional responses to Fe deficiency have been extensively characterized, little is known about the role of Fe in regulating protein translation. Previous reports have shown that Fe deficiency leads to a global inhibition of protein synthesis, which is dependent on the TORC1 and Gcn2/eIF2 α pathways [88, 90]. In addition, Fe serves as a cofactor for several enzymes participating in protein translation, including proteins involved in modifications of factors affecting translation elongation, post-transcriptional transfer RNA (tRNA) modifications, translational termination, and ribosome recycling [6, 91, 92]. Moreover, Cth2 has been shown to repress the translation of specific transcripts in response to Fe deficiency [37]. However, changes in protein translation at the genome-wide level and the mechanisms of translational regulation by Fe have not been previously investigated.

In this work, we applied RNA-Seq and ribosome profiling (Ribo-Seq) to yeast cells undergoing adaptation to Fe deficiency to quantitatively measure translational changes genome-wide. At the translation level, we uncovered that Fe depletion leads to specific downregulation of genes involved in Fe-dependent processes, including mitochondrial translation and heme biosynthesis. We further show that this translational regulation is

mediated by Cth1 and Cth2. We find that Fe deficiency also affects global protein translation by dramatically decreasing the activity of the ribosome recycling factor Rli1. Conversely, eliminating Cth1 and Cth2 increased the levels of Rli1 indicating that cells adapt to Fe deficiency by limiting the activity of Rli1 in response to low Fe in a Cth1/2-dependent manner. Our data also demonstrate that Fe deficiency affects transcription of antisense long non-coding RNAs (lncRNAs) that play a regulatory role by repressing cognate sense mRNA translation. Taken together, this study uncovers the role of the RNA-binding proteins Cth1 and Cth2 in the control of protein translation and how Fe regulates protein synthesis at both global and transcript-specific levels.

3.3. Results

Transcriptional and translational responses during the adaptation to iron deficiency.

Previous studies have shown that Fe deficiency in yeast *S. cerevisiae* leads to changes in transcriptional profiles [12, 87, 93]. In addition, prolonged Fe deficiency has been shown to induce global inhibition of protein synthesis, which is dependent on the Gcn2/eIF2 α pathway [90]. However, little is known about how Fe deprivation manifests at the level of translational regulation. To distinguish the effects of Fe deficiency on mRNA abundance from its effects on protein translation, we performed RNA-Seq and ribosome profiling (Ribo-Seq) in wild-type W303a yeast cells cultured in Fe-sufficient (+Fe) or Fe-deficient conditions (-Fe), achieved by the addition of the Fe²⁺-specific chelator bathophenanthroline disulfonate (BPS). For this, exponentially growing cells were isolated under Fe-sufficient

conditions, and exposed to a short- (3 h) or long-term (6 h) Fe deficiency (Figure 9A). In addition to wild-type cells, we monitored genome-wide transcriptional and translational changes upon Fe limitation in the *cth1Δcth2Δ* mutant. The RNA-Seq and Ribo-Seq profiles showed significantly altered gene expression patterns during adaptation to low Fe from 0 h to 6 h of Fe deficiency, with intermediate changes at 3 h (Figure 8).

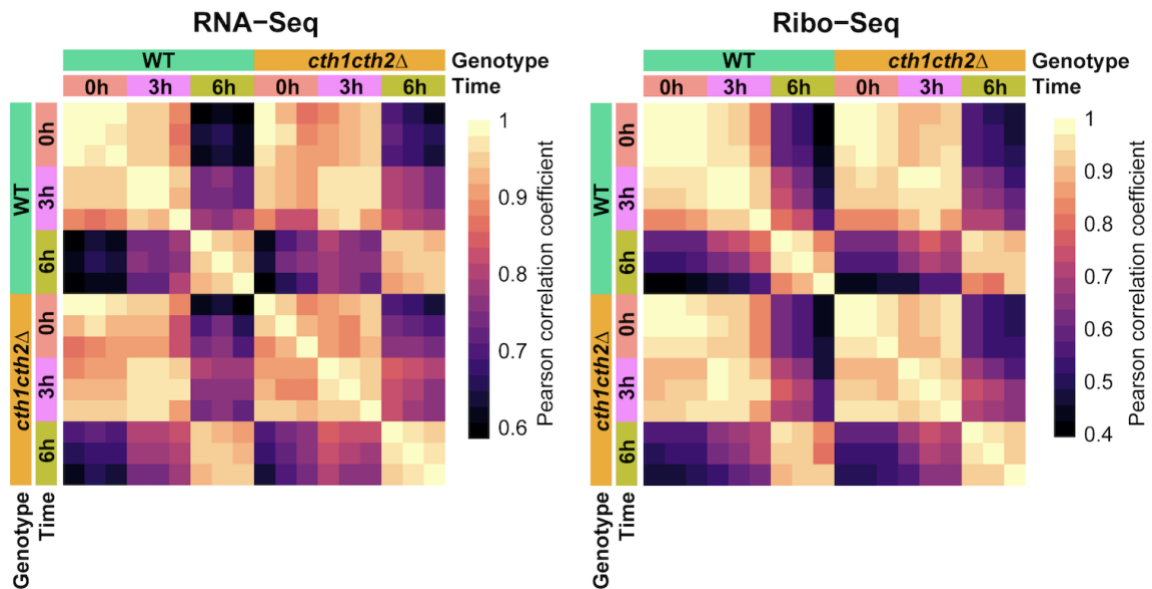


Figure 8. Heatmaps of Pearson correlation coefficients for RNA-Seq and Ribo-Seq replicates in wild-type cells and the *cth1Δcth2Δ* mutant in response to Fe deficiency.

Consistent with previous studies, we also observed strong inhibition of global protein synthesis after 6 h of Fe deficiency in both wild-type cells and the *cth1Δcth2Δ* mutant as measured by polysome analysis, but changes at 3 h were less pronounced (Figure 9B). We found that most of the changes in translation (Ribo-Seq) during Fe deficiency correlated with the changes in mRNA abundance (RNA-Seq) (Figure 9C). Our data demonstrate that the responses to Fe deficiency are mediated primarily by changes in mRNA levels. However, we also found a group of genes that were altered specifically at the translation level indicating that an additional level of regulation contributes to the response of yeast

cells to low Fe (Figure 9D). Specifically, we identified 516 upregulated and 428 downregulated genes, respectively, that were altered exclusively at the translation level in wild-type cells during 6 h Fe deficiency.

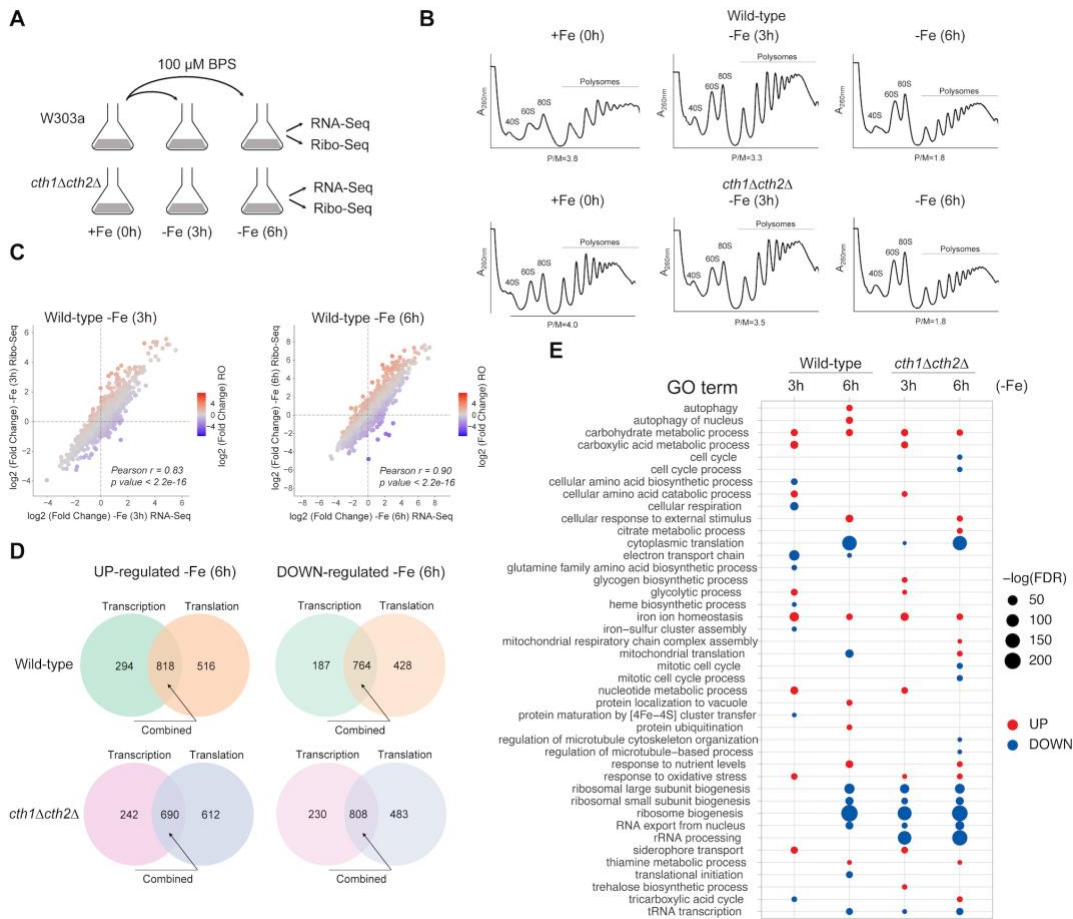


Figure 9. Coordinated changes in mRNA levels and translation allow metabolic reprogramming in response to low Fe

A) Experimental design. **B)** Polysome profiles of wild-type and *cth1 Δ cth2 Δ* cells during the time-course of Fe deficiency. Polysome to monosome (P/M) ratios were calculated using areas under the curve using ImageJ. Corresponding monosome (40S, 60S, 80S) and polysome peaks are indicated. **C)** Comparison of transcriptional (RNA-Seq) and translational (Ribo-Seq) changes during the course of Fe deficiency. Genes whose ribosome occupancy (RO) is increased (red) or decreased (blue) during Fe deficiency are highlighted. **D)** Transcriptional and translational changes in response to Fe deficiency. Venn diagrams show genes that were significantly upregulated or downregulated during 6 h Fe deficiency (FDR<0.05) at the level of mRNA transcription (as quantified by RNA-Seq), translation efficiency or a combined effect. **E)** GO terms enriched among translationally up- and downregulated genes during Fe deficiency.

Our analysis of the RNA-Seq and Ribo-Seq data revealed many of the previously known changes in response to Fe deficiency. Among the genes transcriptionally upregulated during the time-course of Fe deficiency, we observed a number of Fe regulon genes that are controlled by the Aft1 and Aft2 transcription factors, which validated our experimental approach [38, 94]. Genes upregulated in response to short-term (3 h) Fe limitation were enriched in the GO categories “iron ion homeostasis”, “carboxylic acid metabolic process”, “nucleotide metabolic process”, “siderophore transport”, “cellular amino acid catabolic process”, “carbohydrate metabolic process”, “glycolytic process”, and “response to oxidative stress” (Figure 9E). For example, expression of genes involved in Fe siderophore uptake (*FIT1-3*, *ARN1-4*), reductive Fe uptake (*FRE1-FRE4*, *FET3*, *FTR1*, *ATX1*, *CCC2*, *FET4*), and mobilization of vacuolar Fe (*FRE6*, *FET5*, *FTH1*, *SMF3*) increased several folds in response to Fe deprivation in wild-type cells (Figure 10). We also observed that the expression levels of *CTH2*, a gene coding for the mRNA-binding protein involved in metabolic remodeling in response to low Fe, were significantly induced in wild-type cells during Fe deficiency. In addition to “iron ion homeostasis” and “carbohydrate metabolic process”, the late response (6 h) to Fe deficiency was associated with up-regulation of “autophagy”, “cellular response to external stimulus”, “protein localization to vacuole”, “protein ubiquitination”, “response to nutrient levels”, and “thiamine metabolic process” GO categories.

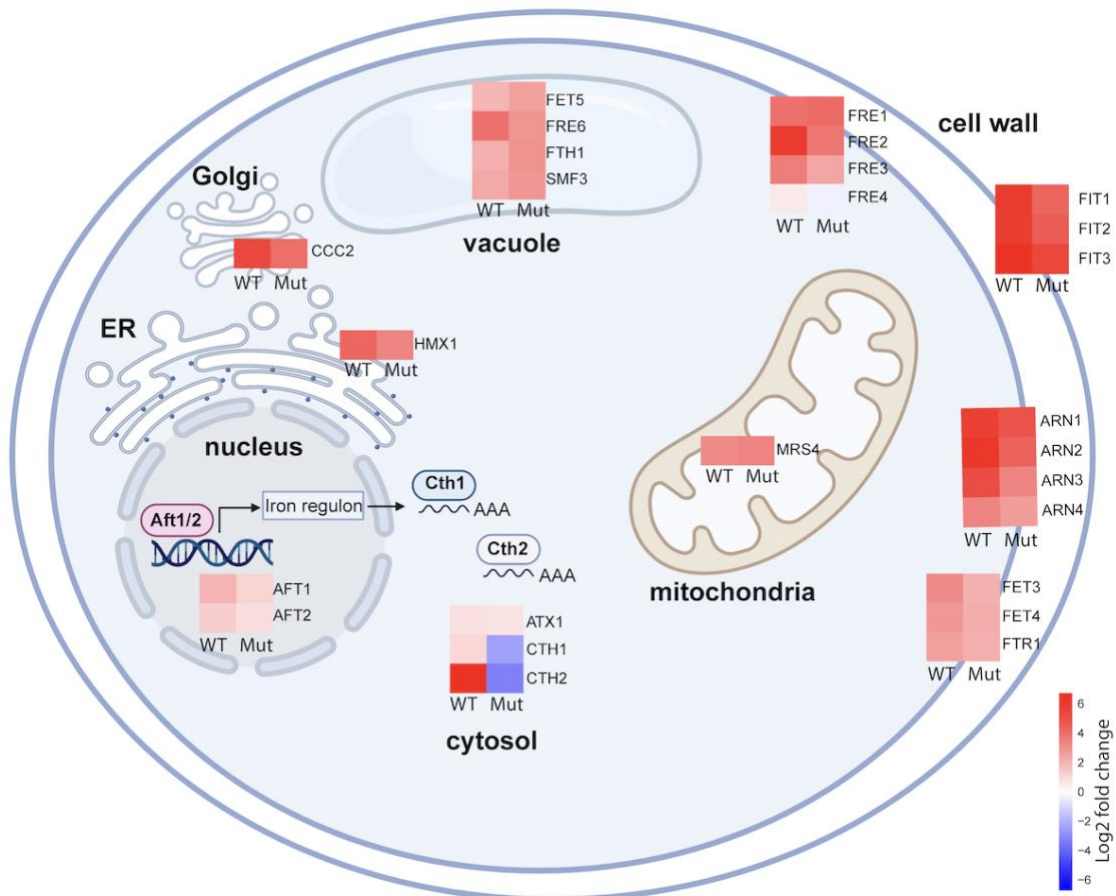


Figure 10. Heatmaps of log₂ fold changes in protein translation (Ribo-Seq) of Fe regulon genes during prolonged (6 h) Fe deficiency in wild-type (WT) cells and the *cth1Δact2Δ* mutant (Mut) (FDR<0.05).

Among downregulated genes in response to prolonged Fe deficiency (6 h) the most enriched GO categories included “ribosome biogenesis”, “cytoplasmic translation”, and “ribosomal large and small subunits” consistent with the overall inhibition of protein synthesis at this timepoint. However, there were substantial differences in downregulated genes between wild-type and *cth1Δact2Δ* cells during both short- (3 h) and long-term (6 h) Fe limitation. For example, “cellular respiration”, “electron transport chain”, “heme biosynthetic process”, “iron-sulfur cluster assembly”, “mitochondrial translation”, and “tricarboxylic acid cycle” were enriched among downregulated genes in wild-type cells,

but not in the *cth1Δcth2Δ* mutant. In contrast, “rRNA processing” and “mitotic cell cycle” were specifically downregulated in the *cth1Δcth2Δ* cells suggesting a role of Cth1 and Cth2 in regulation of these processes.

Ribo-Seq analyses reveal the role of the RNA-binding proteins Cth1 and Cth2 in translational regulation.

During Fe deficiency, yeast cells activate the expression of Cth2, an mRNA-binding protein involved in the remodeling of Fe metabolism. In response to low Fe, Cth2 and, to a lower extent, Cth1 post-transcriptionally inhibit the expression of several mRNAs that contain AU-rich elements (AREs) in the 3'UTR [12, 37]. We expected that the lack of Cth1 and Cth2 in the *cth1Δcth2Δ* mutant would lead to the derepression of their targets. By comparing changes in actively translated mRNAs (Ribo-Seq) in wild-type and *cth1Δcth2Δ* cells, we identified 164 genes that were upregulated in the *cth1Δcth2Δ* mutant compared to wild-type cells during 6 h of Fe deficiency (FDR<0.05) (Figure 11A and Table 2). We further compared changes in ribosomal footprints with changes in RNA abundance allowing us to identify genes that are changed specifically at the translational level. Out of 164 genes upregulated in the *cth1Δcth2Δ* mutant, 153 genes were altered exclusively at the level of protein translation (Figure 12).

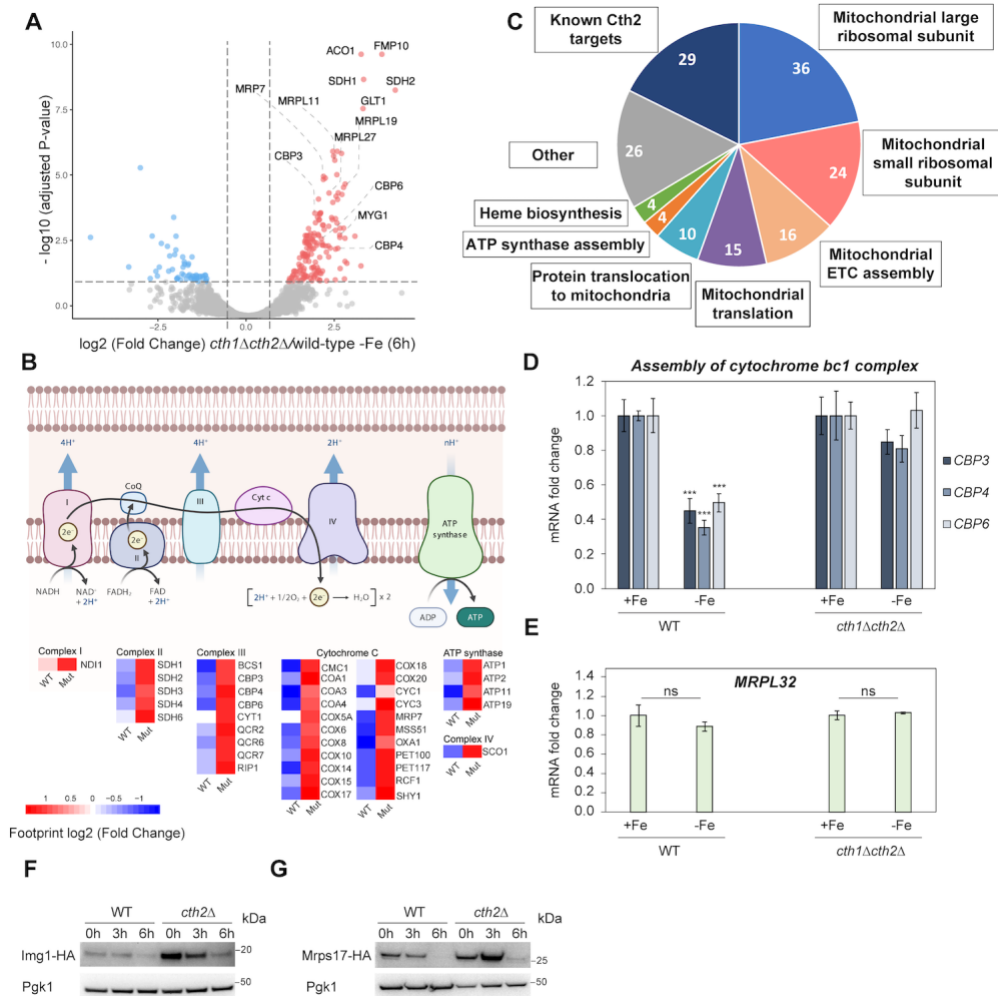


Figure 11. Fe deficiency leads to Cth1/2-dependent inhibition of mitochondrial translation.

A) Volcano plot of differentially regulated genes in the *cth1Δcth2Δ* mutant compared to wild-type cells at 6 h (-Fe). **B**) Heatmap of differentially regulated genes of ETC in *cth1Δcth2Δ* (Mut) compared to wild-type (WT) cells during 6 h of Fe deficiency (FDR<0.05). **C**) Pie chart of genes activated in the *cth1Δcth2Δ* compared to wild-type cells. **D**) Fe deficiency coordinately downregulates expression of transcripts encoding the Cbp3-Cbp4-Cbp6 complex. The expression of *CBP3*, *CBP4*, and *CBP6* was determined by RT-qPCR. Error bars represent SEM of three independent experiments, ****p*<0.001 (one-way ANOVA). **E**) Translation of mitochondrial ribosomal proteins is regulated by Fe deficiency in a Cth1/2-dependent manner without affecting mRNA transcript levels. The expression of *MRPL32* was determined by RT-qPCR. Error bars represent SEM of three independent experiments, ns, non-significant (one-way ANOVA). **F-G**) Lack of Cth2 in the *cth2Δ* mutant leads to derepression of Img1 (**F**) and Mrps17 (**G**) translation. Levels of Img1-HA and Mrps17-HA proteins during Fe deficiency were analyzed by Western blot with anti-HA antibodies. Representative images from two independent experiments are shown.

Among these translationally upregulated genes, we found several previously reported targets of Cth1 and Cth2 that code for components of the electron transport chain (ETC) and tricarboxylic acid (TCA) cycle (Figure 11B and Figure 13), consistent with the known function of Cth1/2 mRNA-binding proteins in post-transcriptional regulation of Fe-dependent genes [11, 37].

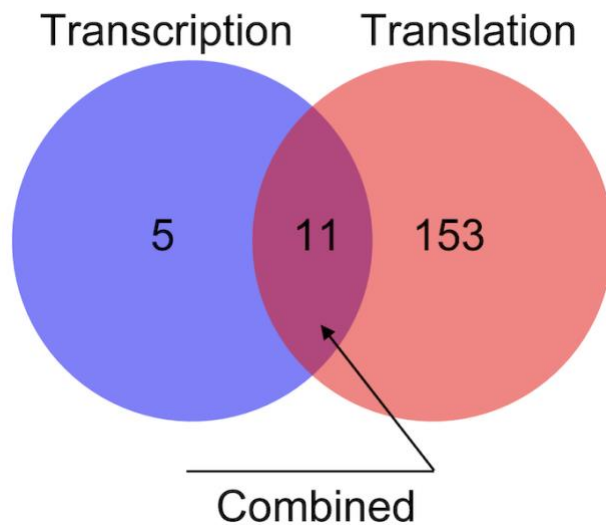


Figure 12. Genes derepressed in *cth1Δcth2Δ* compared to wild-type cells during 6 hours of Fe deficiency.

In addition to previously described Cth1/2 targets, our data uncovered that Cth1 and Cth2 are limiting the expression of genes encoding for mitochondrial ribosomal proteins (MRPs) (36 ribosomal proteins of the large subunit and 24 ribosomal proteins of the small subunit) as well as proteins involved in the assembly of the ETC (16 genes), mitochondrial translation (15 genes), protein translocation to mitochondria (10 genes), ATP synthase assembly (4 genes), and heme biosynthesis (4 genes) (Figure 11C).

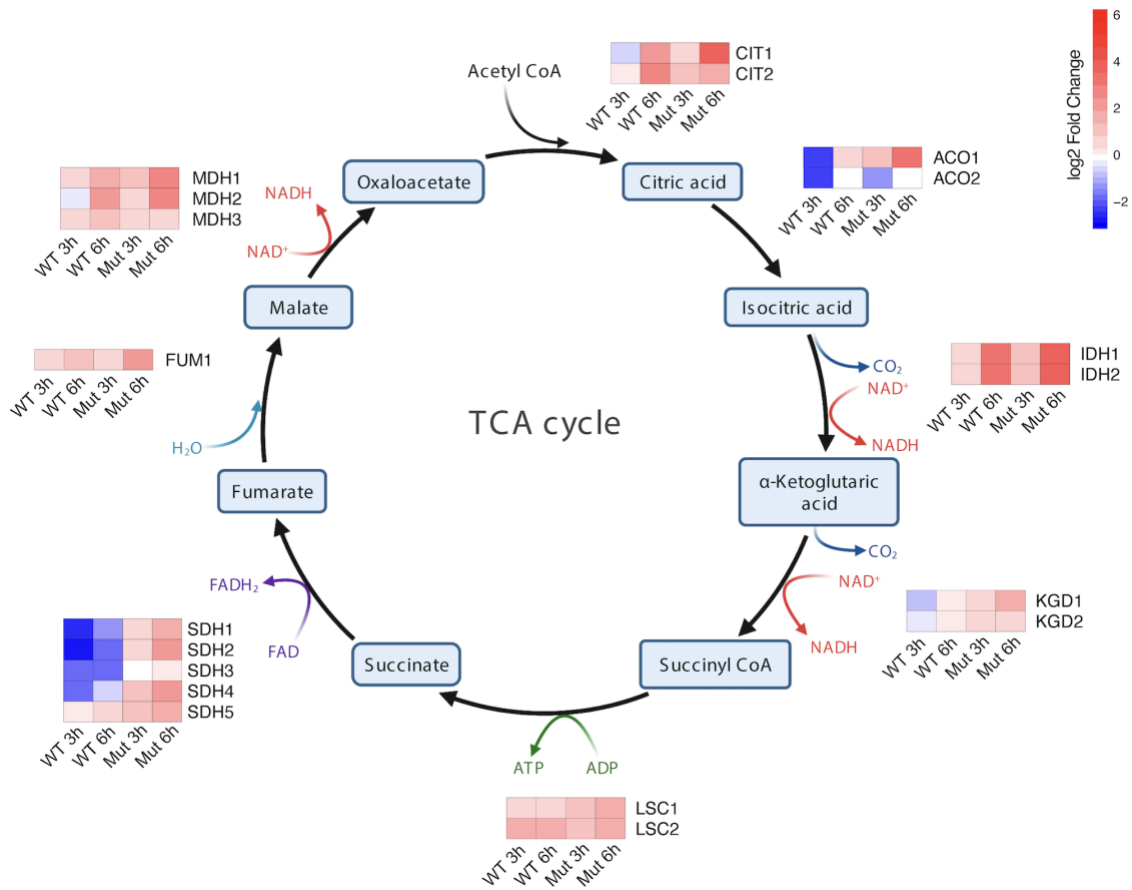


Figure 13. Heatmaps of log₂ fold changes in protein translation (Ribo-Seq) of differentially regulated genes of the TCA cycle during short-term (3 h) and prolonged (6 h) Fe deficiency in wild-type (WT) cells and the *cth1Δcth2Δ* mutant (Mut) (FDR<0.05).

Because known targets of Cth1 and Cth2 contain AREs in their 3'UTR, we searched for putative AREs within 3'UTR of these genes (Table 2). This analysis revealed several transcripts that are directly regulated by Cth1/2. For example, we identified mRNA transcripts encoding the Cbp3-Cbp4-Cbp6 complex, which is involved in the translation and assembly of the mitochondrial cytochrome bc1 complex [95]. Our data demonstrate that *CBP3*, *CBP4*, and *CBP6* are coordinately downregulated in response to low Fe in wild-type cells at the mRNA level (but not in the *cth1Δcth2Δ* mutant), suggesting that *CBP3*, *CBP4*, and *CBP6* are directly regulated by Cth1/2 during Fe deficiency (Figure 11D). In

contrast, most of the genes encoding for MRP proteins lack AREs in their 3'UTRs and Fe deficiency decreased their translation without affecting their transcript levels (Figure 11E and Figure 14).

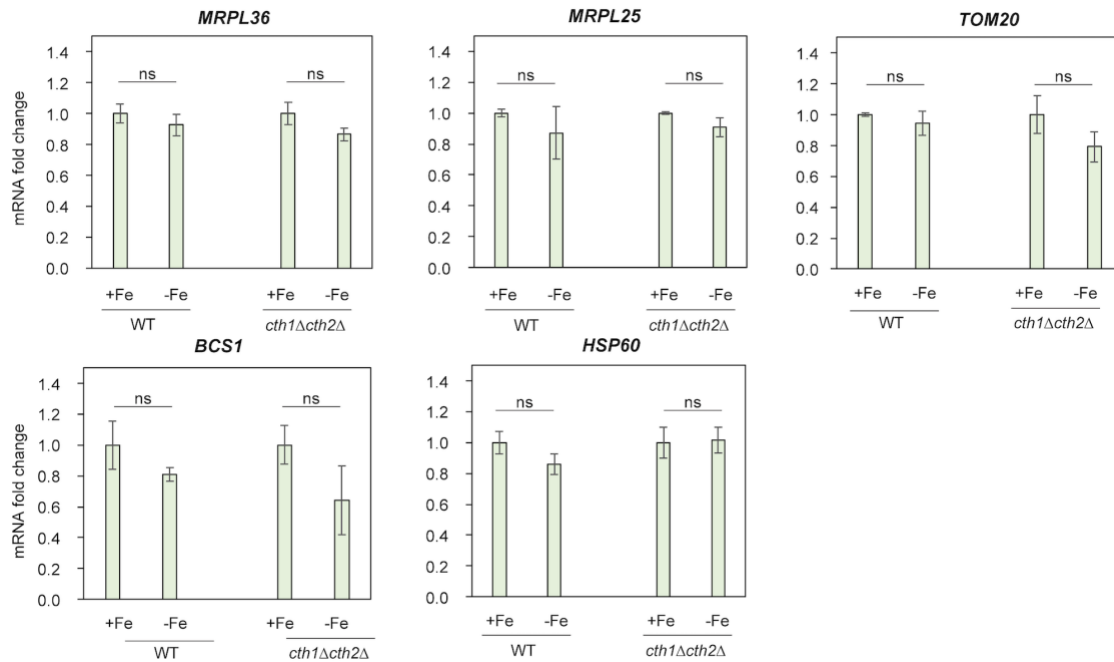


Figure 14. Fe deficiency does not affect transcription levels of mitochondrial ribosomal proteins.

The expression of *MRPL36*, *MRPL25*, *TOM20*, *BCS1*, and *HSP60* was determined by RT-qPCR. Error bars represent SEM of three independent experiments; ns, nonsignificant (one-way ANOVA).

We also observed that expression of Cth1 and Cth2 is reversely correlated with the synthesis of mitochondrial ribosomal proteins of the small subunit (MRPS) and large subunit (MRPL) during the shift of cells from the fermentable carbon source to the non-fermentable medium containing glycerol (Figure 15) that requires the induction of the mitochondrial ETC components and mitochondrial translation [96].

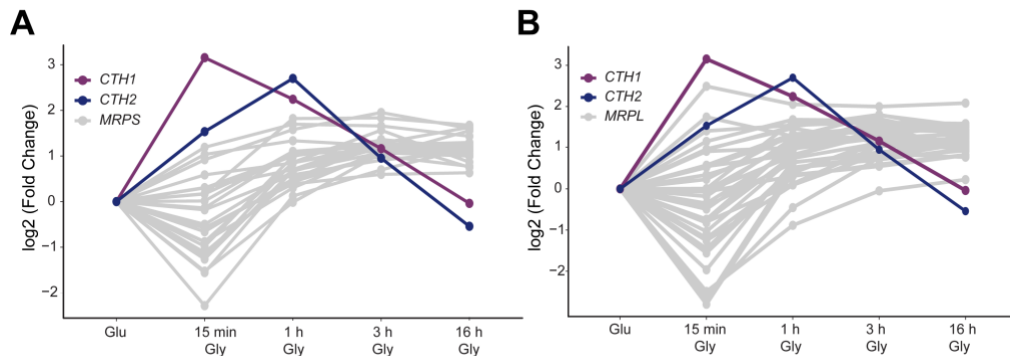


Figure 15. Expression of the mitochondrial ribosomal proteins of the small subunit (A) and large subunit (B) during the shift from the fermentable to non-fermentable carbon source.

Cells were grown in YPD (Glu) medium to log phase and shifted to YPG (Gly) medium or the indicated time. Fold change in protein translation was measured by Ribo-Seq.

Further analysis of MRP genes activated by Fe deficiency in the *cth1Δcth2Δ* mutant identified the presence of Puf3 binding sites in their 3'UTR sequences (Table 2). To validate our findings, we measured the protein levels of two mitochondrial ribosomal proteins, *Img1* and *Mrps17*, regulated by Puf3. Our data show that expression of these targets is downregulated by Fe deficiency. However, the baseline level of both *Img1* and *Mrps17* was significantly higher in the *cth2Δ* mutant compared to wild-type cells (Figure 11F and 11G). These results provide additional support for the role of Cth2 in translational regulation of MRP genes; however, the exact mechanism of this regulation has yet to be investigated.

Notably, we found that Fe deficiency also leads to translational downregulation of genes encoding enzymes involved in heme biosynthesis, including *HEM1*, *HEM3*, *HEM12*, *HEM15* (Figure 16A). To estimate translation efficiency and investigate the contribution of transcriptional and translational regulation to gene expression changes, we calculated

ribosome occupancy (RO) for each of these genes. In wild-type cells, both mRNA abundance (RNA-seq) and protein synthesis (Ribo-Seq) of this set of genes were significantly decreased by Fe deficiency (FDR<0.05). In contrast, translation of *HEM* transcripts was upregulated in the *cth1Δcth2Δ* mutant leading to pronounced increase in RO. To understand whether Cth1 and Cth2 control heme levels, we compared the heme levels in wild-type and *cth1Δcth2Δ* mutant cells subjected to Fe deficiency. We observed a significant decrease in heme levels in wild-type cells after 3 and 6 hours of Fe deficiency, whereas the heme levels in the *cth1Δcth2Δ* mutant cells remained constant (Figure 16B). Together, our results indicate that Cth1 and Cth2 play a central role in controlling the changes in protein translation in response to low Fe by directly and indirectly downregulating multiple transcripts required for mitochondrial translation and heme biosynthesis.

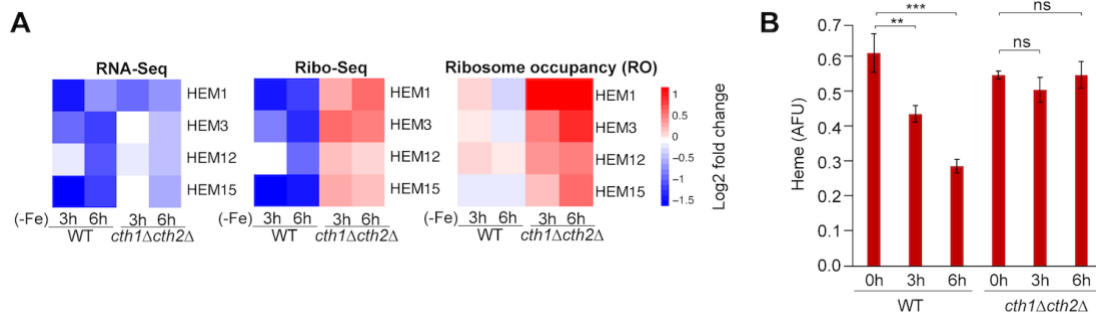


Figure 16. Heme biosynthesis is translationally regulated by Cth1 and Cth2.

A) Heatmaps show log₂ fold change in mRNA abundance (RNA-Seq), protein translation (Ribo-Seq), and ribosome occupancy (RO) compared to untreated (0 h) samples. **B**) Intracellular heme levels decreased significantly during Fe deficiency in wild-type cells, whereas it remained constant in the *cth1Δcth2Δ* mutant. Error bars represent SEM of three biological replicates, each containing two technical replicates. ns, non-significant, **p<0.01, ***p<0.001 compared with wild-type control (two-way ANOVA).

Fe deficiency leads to increased ribosome occupancy in the 3'UTRs of genes due to decreased activity of Rli1.

Although overall protein synthesis is significantly reduced during Fe deficiency, how different steps of protein translation are affected by low Fe is not completely understood. Among enzymes participating in protein translation that require Fe as a cofactor, we selected Rli1 for further analysis. Rli1, the yeast homolog of the mammalian ATP-binding cassette protein E1 (ABCE1), is a key factor in translation termination, ribosome recycling, and translation re-initiation. Rli1 releases ribosomes by promoting the splitting of the 60S ribosomal subunit from the 40S subunit and requires an iron-sulfur (Fe-S) cluster for its activity [6]. *RLI1* mRNA contains two putative AREs within its 3'UTR at 280 and 291 nt from its stop codon, and its transcript levels are upregulated in cells lacking *CTH1* and *CTH2* as compared to wild-type cells in -Fe conditions [11, 12] suggesting it is a direct Cth1/2 target mRNA. We expected that, during Fe deficiency, activity of Rli1 would decrease leading to the increased translation of 3'UTR sequences [91]. To test this, we performed genome-wide quantification of Ribo-Seq reads that aligned to 3'UTR of all annotated genes. We identified numerous 3'UTRs with increased ribosome occupancy in response to Fe deficiency compared to untreated wild-type cells, including *SEDI* and *CWP2*, known targets of Rli1 (Figure 17). Consistent with the function of Rli1 in ribosome recycling, we observed increased accumulation of 80S ribosomes in the 3'UTRs of *SEDI* during prolonged Fe deficiency (6 h) in wild-type cells (Figure 18A).

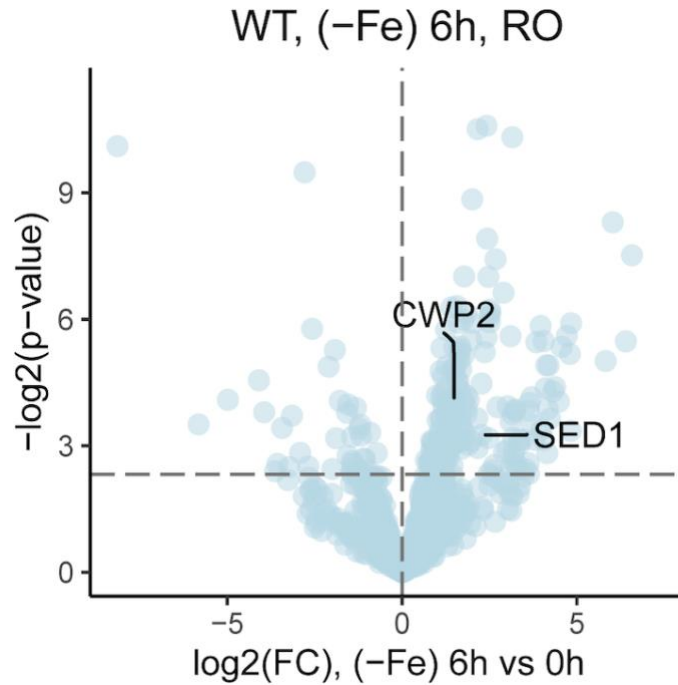


Figure 17. Changes in Ribosome Occupancy (RO) of 3'UTR upon 6 hours of Fe deficiency.

In contrast, the decrease in activity of Rli1 was delayed in the *cth1 Δ cth2 Δ* mutant. To investigate whether increased ribosome occupancy at 3'UTR in Fe-depleted conditions is associated with active translation, we used yeast strains containing 3xHA tags in the 3'UTRs of *SED1* and *CWP2* [91] downstream of the canonical stop codon. We observed increased levels of 3'UTR translation products for *SED1* and *CWP2* genes during prolonged incubation of wild-type cells in the absence of Fe (Figure 18B). Western blot analysis revealed that these bands correspond to the production of small peptide products (~2-5 kDa), rather than read-through translation products that are expected to have larger sizes. Notably, eliminating Cth1 and Cth2 prevented their repressive effects on the expression levels of *RLI1* during Fe deficiency in the *cth1 Δ cth2 Δ* mutant (Figure 18C) lowering expression of the *CWP2* 3'UTR translation product (Figure 18D).

Together, these data suggest that Fe deficiency decreases the activity of Rli1 by promoting binding of Cth1/2 to the AREs in its 3'UTR and promoting degradation of its transcript.

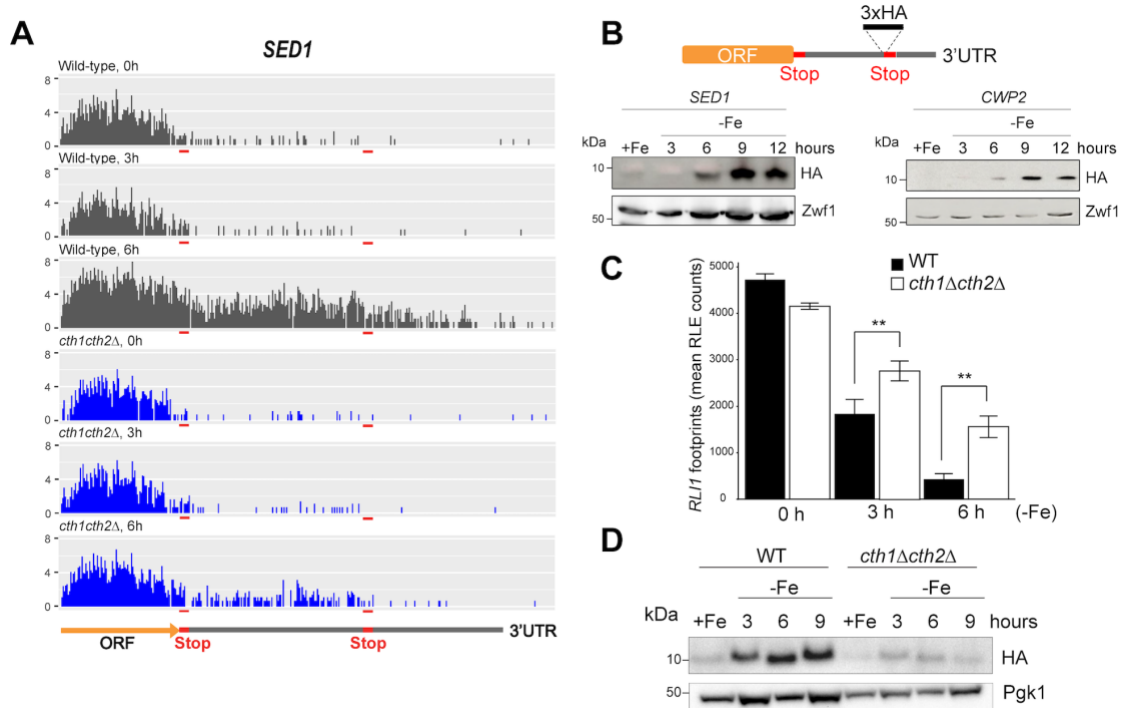


Figure 18. Fe deficiency leads to increased translation of 3'UTRs due to Cth1/2-dependent inhibition of Rli1 activity.

A) Ribosome occupancy at the 3'UTR of *SED1* mRNA during short (3h) and prolonged (6h) Fe deficiency (-Fe). The location of the translation termination site is shown with red boxes. **B)** Strains containing 3xHA tags inserted in the 3'UTRs of *SED1* and *CWP2* [91] show increased translation downstream of the canonical translation stop codon during prolonged Fe deficiency. The expression of tagged proteins was detected by Western blot analysis with HA-tag antibody. Given the size of 4.8 kDa for 3xHA tag, the observed MWs ~7-10 kDa of the bands correspond to the production of small 3'UTR translation products (~2-5 kDa). **C)** Lack of Cth1/2 in the *cth1Δcth2Δ* mutant leads to derepression of *RLI1*. Changes in *RLI1* expression in response to Fe deficiency were calculated by analyzing the number of footprints (RLE normalized counts) in the Ribo-Seq dataset generated in our study. Error bars represent SEM of three independent experiments, ** $p < 0.01$ (one-way ANOVA). **D)** Expression of the *CWP2* 3'UTR translation product is prevented in the *cth1Δcth2Δ* mutant.

MRS3 translation is repressed by antisense transcription of a long non-coding RNA.

Among the genes translationally regulated by Fe deficiency, we identified *MRS3* which encodes a mitochondrial Fe transporter. Footprint coverage of *MRS3* was downregulated in response to Fe deficiency suggesting reduced translation of this gene in low Fe conditions (Figure 19A, right panel). However, at the RNA level, we observed increased expression of an antisense long non-coding RNA (lncRNA), which we named *MRS3^{AS}* (Figure 19A, left panel). We further confirmed increased expression of the *MRS3^{AS}* antisense transcript using RT-qPCR during prolonged Fe deficiency (Figure 19B), which was associated with a 9.2-fold reduction of the Mrs3 protein levels (Figure 19C). In contrast to *MRS3*, low Fe did not affect the footprint coverage of its homolog *MRS4*, and we did not observe the expression of the antisense RNA for this gene (Figure 20A). We then asked whether the increased expression of the *MRS3^{AS}* transcript is dependent on Cth1 and Cth2. However, we observed increased *MRS3^{AS}* transcription in response to low Fe in the *cth1Δcth2Δ* mutant (Figure 20B), indicating that Fe deficiency regulates Mrs3 levels in a Cth1/2-independent manner. Finally, to determine if *MRS3^{AS}* transcription is sufficient for repressing *MRS3*, we generated a plasmid expressing antisense lncRNA. Expression of the full-length *MRS3^{AS}* lncRNA, but not its shorter forms, decreased Mrs3 protein translation in the absence of Fe deficiency (Figure 19D) suggesting that ectopic expression of the antisense lncRNA is sufficient to repress protein translation.

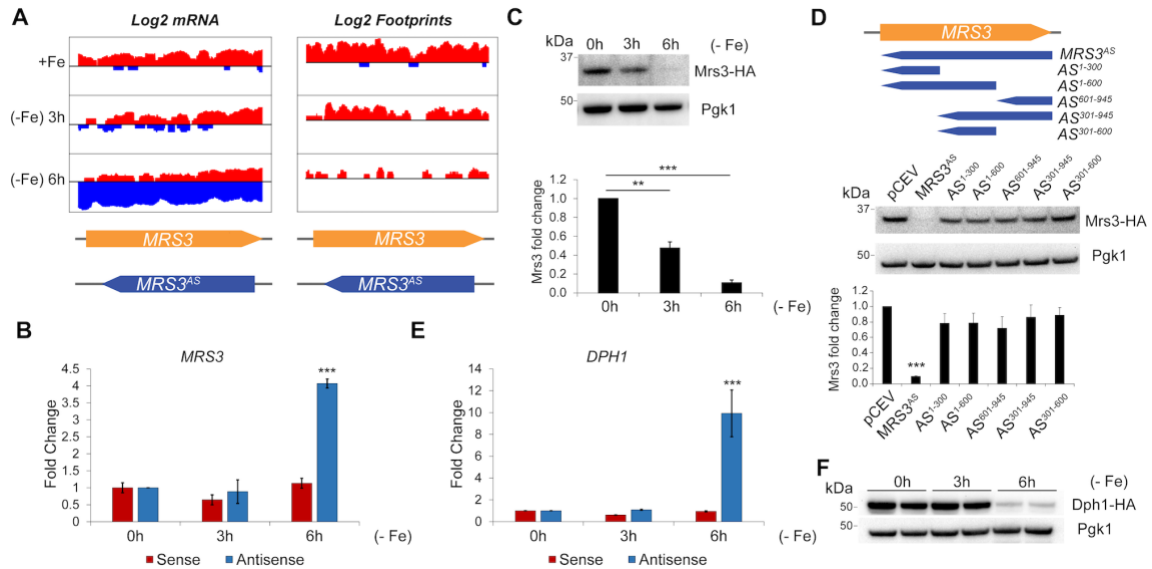


Figure 19. Fe deficiency induces expression of regulatory lncRNAs.

A) Coverage plot of reads mapped to sense (red) and antisense (blue) *MRS3* transcript. Y-axis represents log₂ transformed number of reads, x-axis coordinates show nucleotide positions within *MRS3* ORF. **B**) Expression of antisense *MRS3* (*MRS3^{AS}*) transcript is significantly upregulated upon Fe deficiency. Relative expression of *MRS3* and *MRS3^{AS}* transcripts was analyzed by RT-qPCR. Error bars represent SEM of three independent experiments, ***p<0.001 (two-way ANOVA). **C**) Mrs3 protein levels are repressed by prolonged Fe deficiency. Expression of Mrs3-HA and Pgk1 proteins was determined by Western blot with anti-HA and anti-Pgk1 antibodies, respectively. Error bars represent SEM of three independent experiments, **p<0.01, ***p<0.001 (t-test). **D**) Expression of *MRS3^{AS}* lncRNA is sufficient to repress translation of *MRS3*. Cells expressing HA-tagged Mrs3 protein were transformed with either an empty vector (pCEV) or pCEV-*MRS3^{AS}* expressing full length (*MRS3^{AS}*) or short forms of the antisense *MRS3* transcript (*AS*) and Mrs3 protein levels were analyzed by Western blot. Error bars represent SEM of three independent experiments, ***p<0.001 (t-test). **E**) Relative expression of *DPH1* and *DPH1^{AS}* transcripts was analyzed by RT-qPCR. Error bars represent SEM of three independent experiments, ***p<0.001 (two-way ANOVA). **F**) Expression of Dph1-HA protein during Fe deficiency was analyzed by Western blot with anti-HA antibodies.

Expression of antisense lncRNAs is a conserved regulatory mechanism in yeast.

As *MRS3* is translationally regulated by an antisense lncRNA, we asked if other genes might be controlled by low Fe using a similar mechanism. We searched for the presence of antisense lncRNA transcription in other genes that are translationally downregulated by Fe deficiency. For this, we systematically searched for cis-antisense

transcripts, which overlap protein coding genes and are transcribed from the opposite DNA strand, leading to decreased sense mRNA translation. Using our pipeline, we identified 42 putative mRNA:lncRNA pairs, which had more than a 2-fold increase in expression of antisense transcripts during 6 hours Fe deficiency.

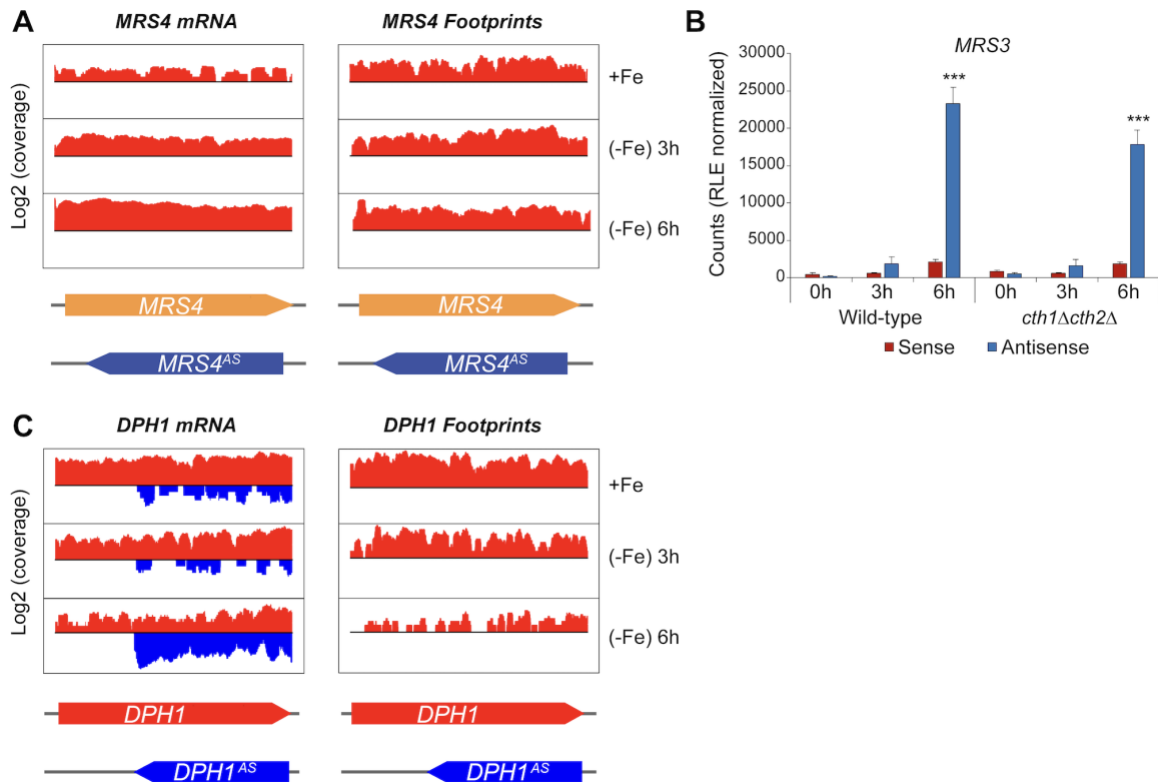


Figure 20. Expression of antisense lncRNA is a conserved regulatory mechanism in yeast.

A) Coverage plot of mRNA and footprint reads mapped to sense (red) and antisense (blue) *MRS4* transcript. B) Expression of antisense *MRS3* (*MRS3*^{AS}) transcript during Fe deficiency is independent of Cth1 and Cth2. Relative expression of *MRS3* and *MRS3*^{AS} transcripts was analyzed by RT-qPCR. Error bars represent SEM of three independent experiments, ****p*<0.001 (two-way ANOVA). C) Fe deficiency induces expression of antisense *DPH1* (*DPH1*^{AS}) transcript. Figure shows coverage plots of mRNA and footprint reads mapped to sense (red) and antisense (blue) *DPH1* transcript.

In addition to *MRS3*, we identified *DPH1*, a Fe-S cluster-containing protein implicated in diphthamide modification of eukaryotic elongation factor 2 (eEF2), which showed increased antisense transcription following 6 h of Fe deficiency (Figure 20C), leading to a

significant decrease of *DPHI* footprint coverage. Using RT-qPCR, we further confirmed the increased expression of the antisense lncRNA (*DPHI^{AS}*) during prolonged Fe deprivation (Figure 19E), which was associated with decreased translation of the main ORF transcript and decreased levels of Dph1 protein (Figure 19F). The observation that translation of both *MRS3* and *DPHI* is repressed by low Fe suggests that this may be a conserved regulatory mechanism.

3.4. Discussion

Although transcriptional responses to Fe deprivation have been extensively characterized, how Fe deficiency affects protein synthesis at the genome-wide level remained elusive. By combining RNA-Seq with the analysis of ribosome occupancy by Ribo-Seq, we quantitatively analyzed translational changes in response to the short-term and prolonged Fe deficiency in yeast. This allowed us to identify groups of genes whose expression was specifically altered by low Fe either at the transcriptional or protein synthesis level, providing mechanistic insights into the role of Fe in protein translation.

The changes in gene expression that we observed were consistent with prior studies that analyzed transcriptomic profiles during Fe deprivation showing altered expression of genes involved in Fe acquisition and mobilization [12, 87]. Expression of these genes is activated by the Aft1 and Aft2 transcription factors. In addition, we observed that Cth1 and Cth2 mRNA-binding proteins repress expression of their targets adjusting metabolism to prioritize Fe for essential processes [94]. For most of the transcripts, a strong correlation between RNA-Seq and Ribo-Seq profiles was found indicating that changes in gene expression induced by Fe deficiency predominantly occur at the mRNA level. However,

we also identified a number of genes that were specifically downregulated by Fe deficiency at the translation level. These downregulated proteins included enzymes involved in heme biosynthesis, as well as mitochondrial ribosomal proteins and other components of the mitochondrial translational machinery. Importantly, we identified Cth1 and Cth2 as key factors responsible for this translational repression. Although *HEM15* was already identified as a target of translational repression by Cth2 in our previously published study [37], we now show that Cth1/2-mediated translational repression of heme biosynthesis genes and inhibition of mitochondrial translation contribute to reducing heme levels in response to Fe deficiency.

Although the exact mechanisms of translational regulation by Cth1 and Cth2 remain unclear, we found that many of the genes translationally downregulated by Cth1/2 contained binding sites for the Puf3 RNA-binding protein in their 3'UTRs. Puf3 is a known regulator of mitochondrial translation in response to glucose availability, which specifically binds to mRNA and represses the translation of mitochondrial ribosomal proteins (MRPs) [54, 97]. In glucose-replete conditions, Puf3 degrades mRNA of MRPs, limiting mitochondrial translation [98, 99], which aligns with known metabolism preferences of yeast for glucose utilization through fermentation. In contrast, glucose depletion or switch to non-fermentable carbon sources leads to Puf3 phosphorylation and the subsequent switch of its function from mRNA degradation to the facilitation of translation [100]. Our data indicate that the expression of Cth1 and Cth2 is inversely correlated with the levels of mitochondrial ribosomal proteins during the transition of yeast cells from high glucose media to media containing glycerol, further supporting the role of

Cth1 and Cth2 in the regulation of mitochondrial translation. Nonfermentable carbon sources, such as glycerol, require the expression of the components of the oxidative phosphorylation and active mitochondrial translation [101], suggesting that the activity of Cth1/2 and Puf3 may allow proper synchronization between mitochondrial translation and Fe levels and that this regulation is not only involved in acute response to Fe deficiency, but may also play a role in physiological, homeostatic processes. Supporting this idea, we recently found that increased expression of Cth2 is limiting the expression of mitochondrial ribosomal proteins during yeast replicative aging [102].

Another effect of Fe deficiency on translation was identified when 3'UTR sequences were analyzed. Ribosome profiling of Fe-depleted cells revealed a striking decrease in the activity of the Fe-S cluster-containing Rli1 protein that serves as a ribosome recycling factor. We show that the number of footprints mapped to 3'UTR sequences was increased in Fe-deficient conditions to the same extent as seen previously in Rli1-depleted yeast cells [91] leading to the generation of aberrant 3'UTR translation products. Notably, we observed a delayed response in the *cth1 Δ cth2 Δ* mutant indicating that Fe deficiency represses Rli1 function in wild-type cells as a result of Cth1/2-mediated post-transcriptional downregulation of *RLI1* transcripts. These data suggest that yeast cells deliberately downregulate the abundance of *RLI1* mRNA through Cth1 and Cth2 to limit Fe utilization by Rli1.

Finally, our study uncovered an important role of antisense lncRNA in the translational regulation of specific mRNA transcripts in response to low Fe. Our data demonstrate that Fe deficiency leads to increased expression of the regulatory antisense

MRS3 transcript repressing translation of cognate mRNA. Moreover, overexpression of the antisense lncRNA is sufficient to repress *Mrs3* translation. Additionally, we found that *Dph1*, a Fe-S cluster-containing protein that participates in the first step of diphthamide modification of eEF2, is also regulated by a lncRNA. Diphthamide modification of eEF2 is important for efficient ribosome translocation and translational fidelity during protein synthesis [6]. Together, these observations suggest a possible mechanism for the role of Fe in global regulation of protein translation and highlight the complexity of the cellular adaptation to low Fe.

Recent genome-wide studies identified a number of genes that have overlapping antisense RNA transcripts in yeast and other species [103-105] raising a possibility that expression of lncRNAs may have a role in Fe-dependent regulation of gene expression in higher eukaryotes. Additionally, regulation of protein translation by antisense transcripts has been implicated in several human diseases including cancer, cardiovascular and muscular pathologies, neurodegenerative disorders, and diabetes [106]. It would be interesting to examine the importance of lncRNA-mediated translational repression in response to Fe deficiency in these pathophysiological processes.

Limitations of the study

Together, our findings uncovered a complex effect of Fe deficiency on the regulation of protein synthesis showing how this important metal affects protein translation

at multiple levels (Figure 21). However, several important questions remain.

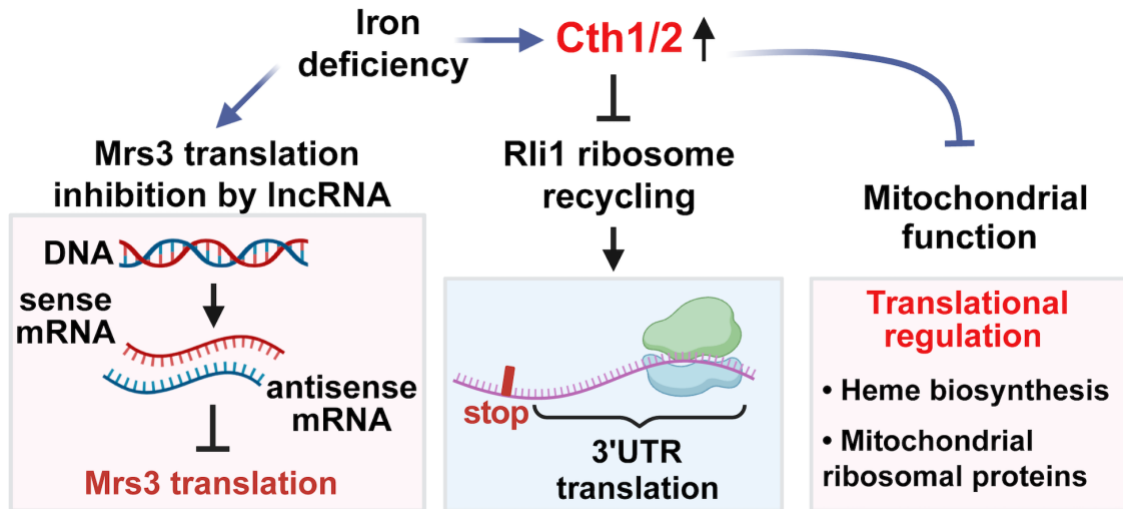


Figure 21. Model for the role of yeast RNA-binding proteins Cth1 and Cth2 in the control of protein translation during adaptation to Fe deficiency.

First, the mechanism by which Cth1 and Cth2 affect translation of mitochondrial ribosomal proteins and the role of Puf3 in this process warrant further investigation. Second, the mechanism of Mrs3 translation inhibition by antisense lncRNA is not completely understood. Future studies will be focused on studying the mechanism underlying the transcriptional activation of *MRS3^{AS}* during periods of Fe deficiency, examining the impact of prolonged Fe deficiency on the transcription of lncRNAs, and gaining a deeper understanding of how this regulatory mechanism contributes to cellular adaptation to Fe deficiency. In this paper we employed a quantitative approach to analyze genome-wide changes in ribosome occupancy of actively translated mRNAs during Fe deficiency in yeast. Nevertheless, the role of mammalian counterparts of Cth2 in regulating protein translation and responding to Fe deficiency remains to be elucidated. Given that many essential Fe-containing enzymes have been implicated in several steps of protein

translation in mammals [6], the principles of Fe-dependent translational regulation uncovered in yeast may shed light on mechanisms that control protein synthesis in higher eukaryotes.

3.5. Methods

Experimental model

One-step polymerase chain reaction (PCR)-mediated gene disruption was performed using standard techniques to delete genes of interest. The genotypes of the resulting strains were verified using colony PCR. Prototroph W303a (*MATa*, *HIS3*, *TRP1*, *LEU2*, *URA3*, *ADE2*, *can1*) and W303a *cth1Δcth2Δ* (*cth1Δ::hphB*, *cth2Δ::KanMX*) cells were cultured at 30°C in liquid SD medium (0.17% yeast nitrogen base without ammonium sulfate and without amino acids, 2% D-glucose, and 2 g/L Kaiser drop-out (Formedium)). For induction of Fe deficiency, cells were initially grown to $OD_{600} = 0.2$ and Fe²⁺ chelator bathophenanthrolinedisulfonic acid (BPS) was added to the final concentration 100 μM. Following the addition of BPS, cells were incubated for 3 h and 6 h. Cells were collected by rapid filtration through 0.45 μm membrane filters using a glass holder filter assembly, scrapped with a spatula, and flash frozen in liquid nitrogen. Yeast strains encoding HA-tagged Mrs3 and Dph1 proteins were generated using CRISPR/Cas9 genome editing [107].

Ribo-Seq and RNA sequencing, data processing, and analysis

Yeast extracts were prepared by cryogrinding the cell paste with BioSpec cryomill. The cell paste was re-suspended in lysis buffer (20 mM Tris-HCl pH 8, 140 mM KCl, 5mM MgCl₂, 0.5 mM DTT, 1% Triton X-100, 100 μg/mL cycloheximide), spun at 20,000 x g at 4°C for 5 min and 1 mL of the supernatant was divided into two tubes, for total mRNAs

and footprint extraction. For Ribo-Seq, 50 OD₂₆₀ units of the lysate (in 1 mL of lysis buffer) were treated with 10 µL of RNase I (100 U/µL) for 1 h, with gentle rotation of samples at room temperature. Then, 1 mL of RNase-treated lysate was layered on a sucrose gradient for isolation of monosomes using ultracentrifugation followed by footprint extraction with hot acid phenol method. For RNA-Seq samples, poly(A) mRNA isolation was performed using a poly(A) mRNA isolation kit with subsequent mRNA fragmentation. The RNA-seq and Ribo-Seq libraries were prepared using the ARTseq Ribosome Profiling kit (Illumina) [74] and sequenced using the Illumina HiSeq platform.

For Ribo-Seq data, the adapter sequence was removed using Cutadapt 4.1 [108] and reads less than 23 nucleotides were filtered out. The Ribo-Seq and RNA-Seq reads were aligned to the *S. cerevisiae* genome from the Saccharomyces Genome Database (<https://www.yeastgenome.org/>, release number R64-2-1). Sequence alignment was performed using STAR software 2.7.1a, allowing two mismatches per read [76]. Counts were generated with featureCounts from Rsubread 1.22.2 package [77]. We filtered out genes with low number of reads (less than 10 counts in less than 66.6% of samples) resulting in 5506 detected genes in RNA-Seq and 5069 genes in Ribo-Seq expression matrices. Identification of differentially expressed genes was performed using the generalized linear model of the EdgeR package (GLM, glmFit, glmLRT) with an adjusted p-value cutoff (FDR<0.05) [78].

Ribosome occupancy analysis.

To estimate translational efficiency changes during Fe deficiency, we analyzed ribosomal occupancy (RO), which represents a ratio between ribosomal footprints and mRNA

abundance allowing to identify actively translated transcripts. To calculate RO, genes with low counts (less than 10 counts) were filtered out from RNA-Seq and Ribo-Seq datasets containing raw counts. RNA-Seq and Ribo-Seq data were then RLE normalized (“Relative Log Expression” normalization) using the edgeR package [78] and RO was calculated using the following formula: $\log_2(\text{Ribo-seq counts} + 1) - \log_2(\text{RNA-seq counts} + 1)$. We used Limma R package to estimate the contribution of transcriptional and translational regulation to gene expression changes and identify translationally regulated genes [79, 80].

Quantification of antisense transcripts

To quantify antisense transcripts, sequence reads that align to annotated ORFs and are transcribed from the opposite DNA strand were counted using featureCounts from Rsubread 1.22.2 package [77]. First, we filtered out genes with less than 5 counts in less than 66.6% of samples (an empirically chosen threshold aiming to bring the distribution of the counts closer to normal and preserve the maximum number of genes with minimal variation between replicates). After filtering step, we obtained 726 genes. RLE normalized counts were then used to identify differentially expressed antisense transcripts during Fe deficiency using Limma R package.

Polysome analysis

Polysome analysis was performed according to the previously published protocol [37]. Cells were grown in SC media overnight upon 0.2 OD₆₀₀ density and supplemented with 100 μM of the bathophenanthroline disulfonate (BPS) to induce Fe deficiency. After 3 and 6 hours, cells were treated with 50 μg/mL cycloheximide (CHX) for 5 min and, after lysis, collected and resuspended in 700 μl of lysis buffer [20 mM Tris-HCl, pH 8, 140 mM KCl,

5 mM MgCl₂, 0.5 mM dithiothreitol, 1% Triton X-100, 0.1 mg/mL CHX, and 0.5 mg/mL heparin]. Aliquots of cell extracts containing 8.5 OD₂₆₀ units were loaded on top of sucrose gradients (5-50% wt/wt). The gradients were sedimented at 200000 x g at 4°C in a SW41 rotor (Beckman) for 2 h 40 min. Fractions were analyzed by UV detection at 260 nm.

RT-qPCR

Total RNA was isolated by hot acid phenol extraction. RNA was treated with DNaseI, and 1 µg of RNA was used for cDNA synthesis using SuperScript III reverse transcriptase (Thermo Fisher Scientific) with random hexamer primers according to manufacturer's instructions. mRNA expression was then analyzed by real-time PCR using KAPA SYBR FAST qPCR Master Mix (Kapa Biosystems) and the CFX-96 Touch Real-Time PCR Detection System (Bio-Rad Laboratories). *ACT1* was used as a reference gene for normalization of mRNA expression between genotypes. Results are represented as means ± SEM from three independent experiments.

Western blot analysis

Total protein extracts were prepared using TCA precipitation. 5 OD₆₀₀ units of cells were resuspended in 0.5 mL of 6% TCA, incubated at least 10 min on ice and centrifuged for 5 min at 4°C at maximum speed (~14,000 x g). Next, the pellet was washed twice with acetone and air-dried. The pellet was then resuspended in 250 µL of HU buffer (5 M urea, 50 mM Tris-HCl pH 7.5, 1% SDS, 1 mM PMSF) and samples were homogenized with glass beads by vortexing at maximum speed for 10 x 30 sec. Equal amounts of proteins were resolved in 10% SDS-PAGE gels and transferred to PVDF membrane. Anti-HA-Peroxidase, High Affinity (3F10) rat monoclonal antibody (Roche) was used to detect HA-

tagged proteins. Mouse anti-Pgk1 monoclonal antibody (Life Technologies) and HRP-conjugated secondary anti-mouse antibody (Santa Cruz Biotechnology) were used to detect Pgk1 protein levels as a loading control.

Expression of the *MRS3^{AS}* lncRNA

To generate plasmids that express the *MRS3^{AS}* lncRNA, the sequence containing *MRS3* ORF (or indicated fragments) was PCR amplified from yeast genomic DNA and integrated in reverse orientation under the control of *TEF1* promoter into pCEV plasmid [109] using SpeI and NotI restriction sites. *W303a* yeast cells were transformed with *pCEV-MRS3^{AS}* plasmids and selected on media containing Zeocin at a final concentration of 300 µg/mL. Expression of the antisense *MRS3^{AS}* transcript was verified using RT-qPCR.

Heme quantification

For induction of Fe deficiency, cells were initially grown to $OD_{600} = 0.2$ and Fe^{2+} chelator bathophenanthrolinedisulfonic acid (BPS) was added to the final concentration 100 µM. Following the addition of BPS, cells were incubated for 3 h and 6 h. Intracellular heme levels were assessed using the oxalic acid method. Briefly, overnight yeast cultures were diluted to $OD_{600} = 0.2$ units/mL and grown until cells reached $OD_{600} = 0.8$ units/mL. Subsequently, 8 OD_{600} units of cells were harvested by centrifugation at 2,500 x g, washed with distilled water, and the pellet was resuspended in 500 µL of 20 mM oxalic acid. An additional 500 µL of 2 M oxalic acid was added, and the suspension was divided equally into two tubes. One set of sample tubes was placed in a heating block at 100°C for 45 min, while the other set of samples was kept at room temperature

for the same duration as a baseline. Following incubation, samples were cooled to room temperature, and 100 μ L of suspension was transferred per well into a black-well 96-well plate in duplicates. The fluorescence of porphyrin was measured using a Biotek plate reader with 400 nm excitation and 662 nm emission. Baseline values (from parallel unheated samples in oxalic acid) were subtracted, and the relative fluorescence intensity in arbitrary units (A.F.U.) was plotted.

Quantification and statistical analysis

Statistical analysis was performed using Prism 9.3.1 (GraphPad Software, Inc). Statistical significance of the RT-qPCR data was determined by calculating p values using one-way ANOVA. Error bars represent standard errors of the means (SEM). The information about number of replicates and P values can be found in figure legends. For RNA-Seq and Ribo-Seq analyses, three biological replicates were analyzed per each condition.

CHAPTER 4

Conclusions and Future Directions

4.1. Conclusions

Cth2 impairs replicative lifespan by inhibiting mitochondrial function

Dysregulation of iron homeostasis has been implicated in the pathogenesis of multiple human age-related diseases. However, the molecular mechanisms underlying the role of iron homeostasis in aging remain poorly understood. In this study, we used yeast as a model system to explore translational changes during aging and investigate the role of iron homeostasis in the regulation of lifespan. Despite the overall decrease in translation, our results revealed that aging in *S. cerevisiae* is associated with altered expression of genes involved in iron starvation response that are under the control of the Aft1 transcription factor. We further identified the RNA-binding protein Cth2 among major transcriptional targets activated by Aft1 with aging and demonstrated that Cth2-dependent repression of its target genes mediates the negative effects on lifespan, leading to repression of mitochondrial function.

Taken together, our findings suggest that Cth2 is a negative regulator of lifespan, which accumulates with aging and down-regulates its downstream targets leading to Cth2-dependent inhibition of mitochondrial respiration. These findings revealed Cth2's critical role in lifespan regulation and suggested that targeting iron homeostasis could be a promising strategy to delay aging.

Cth2-dependent effects of iron deficiency on protein translation

The genome-wide translational response to iron deficiency remains poorly characterized. To address this gap, we examined transcriptional and translational changes in yeast using RNA-Seq and ribosome profiling during short-term (3 hours) and long-term (6 hours) iron deficiency. Our results demonstrated a coordinated transcriptional and translational response to iron depletion. However, we identified a subset of genes that were downregulated specifically at the translational level. This subset included genes encoding mitochondrial ribosomal proteins, mitochondrial translation factors, heme biosynthesis enzymes, and proteins critical for iron homeostasis.

By comparing wild-type and *cth1 Δ cth2 Δ* mutant cells, we identified 153 translational targets of Cth1/2. Notably, these targets include mitochondrial proteins that are also repressed by Cth2 in aging yeast cells. These targets lacked AU-rich elements in 3'UTRs suggesting that Cth2 regulates translation of these genes but not directly. However, analysis of 3'UTRs of these genes revealed the presence of Puf3-binding sites. Puf3, a Pumilio family RNA-binding protein, is known to dynamically regulate mitochondrial ribosomal proteins in response to cellular metabolic states [100, 110]. Our findings suggest that Cth2 may modulate mitochondrial translation indirectly through Puf3.

We further observed that enzymes involved in heme biosynthesis pathway were translationally inhibited under iron-deficient conditions in wild-type cells but not in the *cth1 Δ cth2 Δ* mutant. Correspondingly, intracellular heme levels progressively decreased after 3 and 6 hours of iron deficiency in wild-type cells but remained stable in the mutant cells. Based on these findings, we hypothesized that heme supplementation could positively impact yeast lifespan. Indeed, in our recently published study we found that

heme supplementation extends replicative lifespan in yeast independently of the Hap4 transcription factor and influences mitochondrial respiration [111]. Although the precise mechanism linking Cth2 to heme metabolism remains unclear, these results provide a foundation for future studies of heme supplementation as a novel lifespan-extending intervention.

To investigate the role of Cth2 in global translation regulation under iron deficiency, we focused on the Rli1, an essential ribosome recycling factor and Fe/S cluster-containing protein targeted by Cth2. During iron deficiency, Rli1 levels were reduced, leading to impaired ribosome recycling. This disruption manifested as ribosomal footprint accumulation around stop codons and 3'UTRs in wild-type cells, effects absent in the *cth2Δ* mutant. These findings highlight the role of Cth2 in translation termination and re-initiation under iron-limited conditions. Future studies should explore how Cth2 modulates ribosome recycling and whether peptides synthesized during iron deficiency confer adaptive advantages [112].

Antisense lncRNAs inhibit translation of proteins under iron-deficient conditions

Antisense long non-coding RNAs (lncRNAs) can modulate gene expression at multiple levels, including transcription, translation, and post-transcriptional modifications [113, 114]. This study identified a novel role for antisense lncRNAs in regulating protein translation under iron-deficient conditions. Our analysis revealed 735 genes were associated with differentially expressed antisense lncRNAs under iron-deficient conditions. Among these, 42 antisense lncRNAs exhibited inverse correlations with the translation of their corresponding sense transcripts. For example, we demonstrated that

antisense lncRNA targeting *MRS3* and *DPH1* suppressed protein translation under iron-depleted conditions. These antisense lncRNAs likely act through RNA duplex formation, as their expression levels significantly exceeded that of their sense transcripts during iron deficiency.

4.2. Future Directions

This study highlights the central role of iron in regulating biological processes, particularly in aging and iron deficiency. While yeast has provided a valuable model for understanding translational regulation, genome-wide studies in mammals are needed to assess conservation of these mechanisms.

Future research should focus on the mammalian homologs of Cth2, such as TTP, to explore their potential as therapeutic targets for iron-associated diseases and aging. Additionally, the role of antisense lncRNAs in regulating protein translation under stress conditions offers an intriguing avenue for further investigation, particularly in the context of human health and disease.

By uncovering novel molecular targets and providing insights into the mechanisms underlying iron regulation, this work lays the foundation for the development of innovative therapeutic strategies to treat age-related diseases associated with dysregulated iron homeostasis.

Supplemental Tables

Table 1. Statistical analysis of lifespan experiments.

Figure	Test strain	Test LS	Test cell number	Reference (Ref)	Ref LS	Ref cell number	% Change	p-value
Figure 1B	<i>aft1Δ</i>	1.3	85	WT	21.9	85	-94.1	<0.0001
	<i>ccc1Δ</i>	27.8	80	WT	25.0	80	11.2	0.0582
	<i>cth1Δ</i>	31.5	80	WT	22.7	80	38.8	<0.0001
	<i>cth2Δ</i>	34.3	80	WT	22.7	80	51.1	<0.0001
	<i>fet3Δ</i>	26.1	60	WT	19.6	60	33.2	0.0056
	<i>fit2Δ</i>	23.4	60	WT	19.6	60	19.4	0.0086
	<i>fth1Δ</i>	20.8	60	WT	19.6	60	6.1	0.5374
	<i>grx3Δ</i>	18.3	60	WT	19.6	60	-6.6	0.3036
	<i>hmx1Δ</i>	24.5	60	WT	19.6	60	25.0	0.0006
	<i>isulΔ</i>	17.8	60	WT	19.6	60	-9.2	0.1197
	<i>mrs3Δ</i>	18.7	60	WT	19.6	60	-4.6	0.4529
	<i>vma21Δ</i>	6.4	40	WT	23.7	40	-73.0	<0.0001
Figure 5A	<i>aft1Δ</i>	0.7	45	WT	18.1	45	-96.1	<0.0001
	<i>AFT1-lup</i>	13.8	45	WT	18.1	45	-23.8	0.0017
	<i>cth2Δ</i>	26.2	45	WT	18.1	45	44.8	<0.0001
	<i>AFT1-lup cth2Δ</i>	26.3	45	WT	18.1	45	45.3	<0.0001
	<i>AFT1-lup</i>	13.8	45	<i>cth2Δ</i>	26.2	45	-47.3	<0.0001
	<i>AFT1-lup cth2Δ</i>	26.3	45	<i>cth2Δ</i>	26.2	45	0.4	0.8056
	<i>AFT1-lup</i>	13.8	45	<i>AFT1-lup cth2Δ</i>	26.3	45	-47.5	<0.0001
Figure 6B	<i>cth2Δ</i>	31.4	50	<i>CTH2</i>	25.7	80	22.2	0.0099
	<i>CTH2-C190R</i>	31.2	80	<i>CTH2</i>	25.7	80	21.4	0.0041
	<i>CTH2-S64A,S65A</i>	21.7	83	<i>CTH2</i>	25.7	80	-15.6	0.0231
	<i>CTH2-S64A,S65A ,C190R</i>	26.6	80	<i>CTH2</i>	25.7	80	3.5	0.6219
	<i>CTH2-C190R</i>	31.2	80	<i>CTH2-S64A,S65A</i>	21.7	83	43.8	<0.0001
	<i>cth2Δ</i>	31.4	50	<i>CTH2-S64A,S65A</i>	21.7	83	44.7	<0.0001
	<i>CTH2-C190R</i>	31.2	80	<i>cth2Δ</i>	31.4	50	-0.6	0.7685

Figure 6E	<i>hap4Δ</i>	10.6	80	WT	20.2	80	-47.5	<0.0001
	<i>hap4Δ cth2Δ</i>	20.7	80	WT	20.2	80	2.5	0.7393
	<i>cth2Δ</i>	29.6	80	WT	20.2	80	46.5	<0.0001
	<i>hap4Δ</i>	10.6	80	<i>cth2Δ</i>	29.6	80	-64.2	<0.0001
	<i>hap4Δ cth2Δ</i>	20.7	80	<i>cth2Δ</i>	29.6	80	-30.1	<0.0001
	<i>hap4Δ</i>	10.6	80	<i>hap4Δ cth2Δ</i>	20.7	80	-48.8	<0.0001
Figure 6F	<i>HAP4OE</i>	25.7	160	WT	19.7	120	30.5	<0.0001
	<i>cth2Δ</i>	30.3	120	WT	19.7	120	53.8	<0.0001
	<i>HAP4OE cth2Δ</i>	30.7	120	WT	19.7	120	55.8	<0.0001
	<i>HAP4OE cth2Δ</i>	30.7	120	<i>cth2Δ</i>	30.3	120	1.3	0.9141
	<i>HAP4OE</i>	25.7	160	<i>cth2Δ</i>	30.3	120	-15.2	<0.0001
	<i>HAP4OE</i>	25.7	160	<i>HAP4OE cth2Δ</i>	30.7	120	-16.3	<0.0001

Table 2. Location of putative AU-rich elements (AREs) and Puf3 binding sites in genes translationally regulated by yeast Cth1/Cth2 proteins in response to Fe deficiency, related to Figure 2.

AREs, AU-rich elements (5'-UUUUUU-3' and 5'-UAUUUU-3' octamers) located within 500 nucleotides downstream of the translation termination stop codon. Puf3 sites, predicted 10 nt Puf3 (C/U)(A/C/U)UGUA(A/U)AUA binding elements located within 500 nucleotides downstream of the translation termination stop codon.

Gene	Function	Location of Putative AREs	Location of Puf3 sites
Known Cth2 targets (29)			
<i>ACO1</i>	Aconitase required for the tricarboxylic acid (TCA) cycle	32,150,177	
<i>APE4</i>	Cytoplasmic aspartyl aminopeptidase	33	
<i>CCCI</i>	Vacuolar Fe ²⁺ /Mn ²⁺ transporter	24,144	
<i>CCPI</i>	Mitochondrial cytochrome-c peroxidase	18,41,50,59	
<i>CIR2</i>	Mitochondrial protein with similarity to flavoprotein dehydrogenase	13,37,81	
<i>CLU1</i>	Subunit of the eukaryotic translation initiation factor 3 (eIF3)	23	58
<i>COX10</i>	Heme A:farnesyltransferase		50
<i>DPH2</i>	Protein required for synthesis of diphthamide of translation elongation factor 2		359

<i>FMP10</i>	Protein of unknown function found in mitochondria	15,23	51
<i>GLT1</i>	NAD(+)-dependent glutamate synthase (GOGAT)	15,37,45,53,61,69,77	
<i>ISA1</i>	Protein required for maturation of mitochondrial [4Fe-4S] proteins	46,62	
<i>ILV3</i>	Dihydroxyacid dehydratase involved in biosynthesis of branched-chain amino acids	98	
<i>KGD1</i>	Subunit of the mitochondrial alpha-ketoglutarate dehydrogenase complex	193,230	
<i>LEU1</i>	Isopropylmalate isomerase involved in the leucine biosynthesis pathway	85,123	
<i>LIP5</i>	Protein involved in biosynthesis of the coenzyme lipoic acid	70,92,124	178
<i>NFU1</i>	Protein involved in Fe-S cluster transfer to mitochondrial clients	192,204	52
<i>QCR2</i>	Subunit 2 of the ubiquinol cytochrome-c reductase complex	155	
<i>QCR6</i>	Subunit 6 of the ubiquinol cytochrome-c reductase complex	31	

<i>QCR8</i>	Subunit 8 of the ubiquinol cytochrome-c reductase complex	97,114	
<i>RIP1</i>	Ubiquinol-cytochrome-c reductase	293,355	
<i>RLI1</i>	Essential Fe-S protein required for ribosome biogenesis and translation initiation	280,291	
<i>RNR4</i>	Ribonucleotide-diphosphate reductase (RNR) small subunit	39,125	
<i>SDH1</i>	Flavoprotein subunit of succinate dehydrogenase	153,164,180,188,196,000	97
<i>SDH2</i>	Iron-sulfur protein subunit of succinate dehydrogenase	163,309,328	196
<i>SDH3</i>	Subunit of succinate dehydrogenase	90	
<i>SDH4</i>	Membrane anchor subunit of succinate dehydrogenase	122,136,159	
<i>TRP1</i>	Phosphoribosylanthranilate isomerase	16	315
<i>WTM1</i>	Transcriptional repressor involved in regulation of meiosis, silencing, and expression of RNR genes	145	
<i>YNL320W</i>	Putative protein of unknown function	92	
Mitochondrial ribosomal protein (large subunit) (36)			

<i>IMG1</i>	Mitochondrial ribosomal protein of the large subunit	31
<i>IMG2</i>	Mitochondrial ribosomal protein of the large subunit	30
<i>MHR1</i>	Mitochondrial ribosomal protein of the large subunit	56
<i>MNPI</i>	Mitochondrial ribosomal protein of the large subunit	77,154
<i>MRP7</i>	Mitochondrial ribosomal protein of the large subunit	50
<i>MRPL1</i>	Mitochondrial ribosomal protein of the large subunit	26,85
<i>MRPL3</i>	Mitochondrial ribosomal protein of the large subunit	16,51
<i>MRPL4</i>	Mitochondrial ribosomal protein of the large subunit	26
<i>MRPL6</i>	Mitochondrial ribosomal protein of the large subunit	84
<i>MRPL7</i>	Mitochondrial ribosomal protein of the large subunit	#####
<i>MRPL8</i>	Mitochondrial ribosomal protein of the large subunit	25
<i>MRPL9</i>	Mitochondrial ribosomal protein of the large subunit	31
<i>MRPL10</i>	Mitochondrial ribosomal protein of the large subunit	52
<i>MRPL11</i>	Mitochondrial ribosomal protein of the large subunit	52
<i>MRPL13</i>	Mitochondrial ribosomal protein of the large subunit	45
<i>MRPL15</i>	Mitochondrial ribosomal protein of the large subunit	59
<i>MRPL17</i>	Mitochondrial ribosomal protein of the large subunit	87

<i>MRPL19</i>	Mitochondrial ribosomal protein of the large subunit		85,23
<i>MRPL20</i>	Mitochondrial ribosomal protein of the large subunit		25
<i>MRPL22</i>	Mitochondrial ribosomal protein of the large subunit	259	134
<i>MRPL25</i>	Mitochondrial ribosomal protein of the large subunit		76
<i>MRPL27</i>	Mitochondrial ribosomal protein of the large subunit	2	28
<i>MRPL31</i>	Mitochondrial ribosomal protein of the large subunit		41
<i>MRPL32</i>	Mitochondrial ribosomal protein of the large subunit	75	44,69
<i>MRPL33</i>	Mitochondrial ribosomal protein of the large subunit		56,163
<i>MRPL35</i>	Mitochondrial ribosomal protein of the large subunit		27
<i>MRPL36</i>	Mitochondrial ribosomal protein of the large subunit		#####
<i>MRPL37</i>	Mitochondrial ribosomal protein of the large subunit		31
<i>MRPL40</i>	Mitochondrial ribosomal protein of the large subunit	254	106
<i>MRPL44</i>	Mitochondrial ribosomal protein of the large subunit		86
<i>MRPL49</i>	Mitochondrial ribosomal protein of the large subunit		11,39
<i>MRPL50</i>	Mitochondrial ribosomal protein of the large subunit		35
<i>MRPL51</i>	Mitochondrial ribosomal protein of the large subunit		46
<i>RML2</i>	Mitochondrial ribosomal protein of the large subunit		119

<i>RTC6</i>	Mitochondrial ribosomal protein of the large subunit	64,96
<i>YML6</i>	Mitochondrial ribosomal protein of the large subunit	7,79
Mitochondrial ribosomal protein (small subunit) (24)		
<i>EHD3</i>	Mitochondrial ribosomal protein of the small subunit	54,88
<i>MRP1</i>	Mitochondrial ribosomal protein of the small subunit	49,81
<i>MRP2</i>	Mitochondrial ribosomal protein of the small subunit	48
<i>MRP4</i>	Mitochondrial ribosomal protein of the small subunit	35
<i>MRP13</i>	Mitochondrial ribosomal protein of the small subunit	39
<i>MRP17</i>	Mitochondrial ribosomal protein of the small subunit	39,199
<i>MRP21</i>	Mitochondrial ribosomal protein of the small subunit	52,89
<i>MRP51</i>	Mitochondrial ribosomal protein of the small subunit	28,44

<i>MRPS5</i>	Mitochondrial ribosomal protein of the small subunit		6,68
<i>MRPS8</i>	Mitochondrial ribosomal protein of the small subunit		58
<i>MRPS9</i>	Mitochondrial ribosomal protein of the small subunit		137,330
<i>MRPS12</i>	Mitochondrial ribosomal protein of the small subunit		72
<i>MRPS18</i>	Mitochondrial ribosomal protein of the small subunit		61
<i>MRPS28</i>	Mitochondrial ribosomal protein of the small subunit		27
<i>MRPS35</i>	Mitochondrial ribosomal protein of the small subunit		26,68
<i>NAM9</i>	Mitochondrial ribosomal protein of the small subunit		53
<i>PET123</i>	Mitochondrial ribosomal protein of the small subunit		109
<i>RSM7</i>	Mitochondrial ribosomal protein of the small subunit		20
<i>RSM19</i>	Mitochondrial ribosomal protein of the small subunit	293	8,36

<i>RSM24</i>	Mitochondrial ribosomal protein of the small subunit		31
<i>RSM25</i>	Mitochondrial ribosomal protein of the small subunit		37
<i>RSM26</i>	Mitochondrial ribosomal protein of the small subunit		35,86
<i>RSM27</i>	Mitochondrial ribosomal protein of the small subunit		49,147
<i>RSM28</i>	Mitochondrial ribosomal protein of the small subunit		30
Mitochondrial electron transport chain assembly (16)			
<i>BCS1</i>	Protein required for complex III assembly		27
<i>CBP3</i>	Mitochondrial protein required for assembly of cytochrome bc1 complex III	38	134
<i>CBP4</i>	Mitochondrial protein required for assembly of cytochrome bc1 complex III	80, 248	94
<i>CBP6</i>	Mitochondrial protein required for assembly of cytochrome bc1 complex III	33	21

<i>CMC2</i>	Protein involved in respiratory chain complex assembly		50
<i>COA1</i>	Mitochondrial protein required for assembly of the cytochrome c oxidase complex (complex IV)		22
<i>COA4</i>	win Cx(9)C protein involved in cytochrome c oxidase organization		25
<i>COX14</i>	Mitochondrial cytochrome c oxidase (complex IV) assembly factor		140
<i>COX17</i>	Metallochaperone required for copper delivery to cytochrome c oxidase (complex IV)		30,75
<i>CYT2</i>	Cytochrome c1 heme lyase involved in maturation of cytochrome c1		16
<i>HSP60</i>	Tetradecameric mitochondrial chaperonin		57
<i>MSS51</i>	Specific translational activator for the mitochondrial <i>COX1</i> mRNA		92
<i>PET100</i>	Chaperone that facilitates the assembly of cytochrome c oxidase (complex IV)	55	70
<i>PET117</i>	Assembly factor that couples heme a synthesis to complex IV assembly		46

<i>SCO1</i>	Copper-binding protein required for cytochrome c oxidase (complex IV)	27,66
<i>TCM62</i>	Protein involved in assembly of the succinate dehydrogenase (complex II)	40
Mitochondrial translation (15)		
<i>AIM10</i>	Mitochondrial protein with similarity to tRNA synthetases	31
<i>IFM1</i>	Mitochondrial translation initiation factor 2	102,125
<i>MEF1</i>	Mitochondrial translation elongation factor	25,123
<i>MSD1</i>	Mitochondrial aspartyl-tRNA synthetase	63,92
<i>MSE1</i>	Mitochondrial glutamyl-tRNA synthetase	37
<i>MSK1</i>	Mitochondrial lysine-tRNA synthetase	24,46
<i>MST1</i>	Mitochondrial threonyl-tRNA synthetase	24,106
<i>MSY1</i>	Mitochondrial tyrosyl-tRNA synthetase	24,76
<i>MSC6</i>	Multicopy suppressor of HER2 involved in mitochondrial translation	81
<i>MTO1</i>	Mitochondrial protein involved in mitochondrial tRNA modification	25

<i>MYG1</i>	3'-5' RNA exonuclease involved in regulation of mitochondrial translation	59	
<i>NAM2</i>	Mitochondrial leucyl-tRNA synthetase		31,117
<i>RPM2</i>	Protein subunit of mitochondrial RNase P	19	
<i>RRF1</i>	Mitochondrial ribosome recycling factor		40
<i>TUF1</i>	Mitochondrial translation elongation factor Tu		87,188
Protein translocation to mitochondria (10)			
<i>MBA1</i>	Membrane-associated mitoribosome receptor		6,37,350
<i>MIA40</i>	Component of MIA pathway		54
<i>MSP1</i>	AAA-ATPase involved in mitochondrial protein sorting		101
<i>PAM16</i>	Subunit of the import motor component of the translocase TIM23 complex		110
<i>PAM18</i>	Subunit of the import motor component of the translocase TIM23 complex		126,141
<i>SSCI</i>	Hsp70 family ATPase import motor component of the TIM23 complex		

<i>TAM41</i>	Mitochondrial phosphatidate cytidyltransferase	110	
<i>TIM17</i>	Essential component of the translocase TIM23 complex	309	2,158
<i>TOM20</i>	Component of the TOM complex		47,189
<i>XDJ1</i>	Chaperone involved in mitochondrial protein import		54
ATP synthase assembly (4)			
<i>ATP11</i>	Molecular chaperone required for the assembly of the mitochondrial F1/F0 ATP synthase		54
<i>ATP12</i>	Assembly factor for the mitochondrial F1/F0 ATP synthase		71
<i>ATP2</i>	Beta subunit of the mitochondrial F1/F0 ATP synthase		230
<i>FMCI</i>	Mitochondrial protein required for assembly of the mitochondrial F1/F0 ATP synthase		28,55
Heme biosynthesis (4)			
<i>HAP4</i>	Heme activator protein	275, 304	
<i>HEM1</i>	5-aminolevulinate synthase	103,140	

<i>HEM3</i>	Porphobilinogen deaminase	102,251	263
<i>HEM15</i>	Ferrochelatase, catalyzes the insertion of ferrous iron into protoporphyrin IX	44,100	
Other (26)			
<i>ADH6</i>	NADPH-dependent medium chain alcohol dehydrogenase		135
<i>AIM32</i>	2Fe-2S mitochondrial protein involved in redox quality control	87	
<i>AIM36</i>	Protein of unknown function		53
<i>COQ1</i>	Hexaprenyl pyrophosphate synthetase involved in ubiquinone biosynthesis		79
<i>COQ6</i>	Flavin-dependent monooxygenase involved in ubiquinone biosynthesis	42	5
<i>DPC29</i>	Putative mitochondrial protein of unknown function		40
<i>FLX1</i>	Mitochondrial flavin adenine dinucleotide transporter		31
<i>IBA57</i>	Protein involved in incorporating iron-sulfur clusters into proteins		16
<i>LIP2</i>	Lipoyl ligase		126

<i>MAM33</i>	Protein involved in mitochondrial ribosome assembly		62
<i>MAS2</i>	Alpha subunit of the mitochondrial processing protease		213
<i>MGP12</i>	Mitochondrial glutaredoxin-like protein		29
<i>MIX23</i>	Mitochondrial intermembrane space protein of unknown function		48
<i>MRX15</i>	Membrane-associated mitoribosome receptor		24,61
<i>MRX20</i>	Putative mitochondrial transport protein		26
<i>NAT2</i>	N-terminal acetyltransferase		23
<i>POA1</i>	Phosphatase that is highly specific for ADP-ribose 1"-phosphate	42	
<i>PHB1</i>	Subunit of the prohibitin complex		64
<i>PHB2</i>	Subunit of the prohibitin complex		109
<i>PUF3</i>	mRNA-binding protein involved in regulation of nuclear-encoded mitochondrial proteins		369
<i>RIM2</i>	Mitochondrial pyrimidine nucleotide transporter	164	
<i>RKM5</i>	Protein lysine methyltransferase involved in modification of the		286

	ribosomal large subunit Rpl1a/Rpl1b		
<i>RMD9</i>	Mitochondrial protein that controls mitochondrial gene expression		40,99
<i>YFH1</i>	Mitochondrial matrix iron chaperone	26	
<i>YLF2</i>	Protein of unknown function		17
<i>YML002W</i>	Putative protein of unknown function		

List of Journal Abbreviations

Abbreviation	Complete Journal Title
Aging Cell	Aging Cell
Ann Transl Med	Annals of translational medicine
Annu Rev Genet	Annual review of genetics
Annual Review of Genomics and Human Genetics	Annual Review of Genomics and Human Genetics
Appl Microbiol Biotechnol	Applied microbiology and biotechnology
Biochim Biophys Acta	Biochimica et biophysica acta
Biochim Biophys Acta Gene Regul Mech	Biochimica et biophysica acta. Gene regulatory mechanisms
Bioinformatics	Bioinformatics
Biosci Rep	Bioscience reports
BMC Bioinformatics	BMC Bioinformatics
BMC Genomics	BMC Genomics
Cancer Cell Int	Cancer cell international
Cell	Cell
Cell Chem Biol	Cell chemical biology
Cell Metab	Cell metabolism
Cell Rep	Cell Reports
Cell Syst	Cell systems
Chem Rev	Chemical reviews
Clin Interv Aging	Clinical interventions in aging
Clin Nutr ESPEN	Clinical nutrition ESPEN
CMAJ	Canadian Medical Association journal
Curr Genet	Current genetics
Elife	eLife
EMBO J	The EMBO journal
Eukaryot Cell	Eukaryotic cell
FEBS J	The FEBS journal
Front Microbiol	Frontiers in microbiology
Front Neurosci	Frontiers in neuroscience
Front Pharmacol	Frontiers in pharmacology
Frontiers in Aging Neuroscience	Frontiers in Aging Neuroscience
Frontiers in Molecular Biosciences	Frontiers in Molecular Biosciences
Gene	Gene

Genes Dev	Genes & development
Genetics	Genetics
Genome Biol	Genome biology
Genome Res	Genome research
Geroscience	Geroscience
Hematology Am Soc Hematol Educ Program	Hematology. American Society of Hematology. Education Program
Int J Mol Sci	International journal of molecular sciences
J Biol Chem	The Journal of biological chemistry
J Cell Biol	The Journal of cell biology
J Econ Entomol	Journal of economic entomology
J Neurochem	Journal of neurochemistry
J Vis Exp	Journal of visualized experiments
mBio	mBio
Metallomics	Metallomics
Microb Cell Fact	Microbial cell factories
Microorganisms	Microorganisms
Mol Biol Cell	Molecular biology of the cell
Mol Cell	Molecular Cell
Mol Cell Biol	Cellular and molecular biology
Mol Gen Genet	Molecular & general genetics : MGG
Mol Neurobiol	Molecular neurobiology
Nat Cell Biol	Nature cell biology
Nat Commun	Nature communications
Nat Genet	Nature genetics
Nat Methods	Nature methods
Nature	Nature
Noncoding RNA	Noncoding RNA
Nucleic Acids Res	Nucleic Acids Research
Nutrition	Nutrition
PLoS Biol	PLoS biology
PLoS Genet	PLoS Genetics
Proc Natl Acad Sci U S A	Proceedings of the National Academy of Sciences of the United States of America
Protein & Cell	Protein & Cell
Redox Biol	Redox biology
Rev Neurosci	Reviews in the neurosciences
RNA	RNA

Sci Rep	Scientific Reports
Science	Science
Ther Adv Drug Saf	Therapeutic advances in drug safety
Therap Adv Gastroenterol	Therapeutic advances in gastroenterology
Trends Endocrinol Metab	Trends in endocrinology and metabolism: TEM
World J Microbiol Biotechnol	World journal of microbiology & biotechnology

BIBLIOGRAPHY

1. Andreini, C., et al., *The human iron-proteome*. Metallomics, 2018. **10**(9): p. 1223-1231.
2. Read, A.D., et al., *Mitochondrial iron-sulfur clusters: Structure, function, and an emerging role in vascular biology*. Redox Biol, 2021. **47**: p. 102164.
3. Puig, S., et al., *The elemental role of iron in DNA synthesis and repair*. Metallomics, 2017. **9**(11): p. 1483-1500.
4. Poltorack, C.D. and S.J. Dixon, *Understanding the role of cysteine in ferroptosis: progress & paradoxes*. FEBS J, 2022. **289**(2): p. 374-385.
5. Enko, D., et al., *Branched-chain amino acids are linked with iron metabolism*. Ann Transl Med, 2020. **8**(23): p. 1569.
6. Romero, A.M., M.T. Martinez-Pastor, and S. Puig, *Iron in Translation: From the Beginning to the End*. Microorganisms, 2021. **9**(5).
7. Shin, B.S., et al., *eEF2 diphthamide modification restrains spurious frameshifting to maintain translational fidelity*. Nucleic Acids Res, 2023. **51**(13): p. 6899-6913.
8. Shapiro, J.S., et al., *Iron drives anabolic metabolism through active histone demethylation and mTORC1*. Nat Cell Biol, 2023. **25**(10): p. 1478-1494.
9. Wade, J., et al., *Temporal variation of planetary iron as a driver of evolution*. Proc Natl Acad Sci U S A, 2021. **118**(51).
10. Philpott, C.C. and O. Protchenko, *Response to iron deprivation in Saccharomyces cerevisiae*. Eukaryot Cell, 2008. **7**(1): p. 20-7.
11. Puig, S., S.V. Vergara, and D.J. Thiele, *Cooperation of two mRNA-binding proteins drives metabolic adaptation to iron deficiency*. Cell Metab, 2008. **7**(6): p. 555-64.
12. Puig, S., E. Askeland, and D.J. Thiele, *Coordinated remodeling of cellular metabolism during iron deficiency through targeted mRNA degradation*. Cell, 2005. **120**(1): p. 99-110.
13. McCormick, M.A., et al., *A Comprehensive Analysis of Replicative Lifespan in 4,698 Single-Gene Deletion Strains Uncovers Conserved Mechanisms of Aging*. Cell Metab, 2015. **22**(5): p. 895-906.

14. Manckoundia, P., et al., *Iron in the General Population and Specificities in Older Adults: Metabolism, Causes and Consequences of Decrease or Overload, and Biological Assessment*. Clin Interv Aging, 2020. **15**: p. 1927-1938.
15. Jabara, H.H., et al., *A missense mutation in TFRC, encoding transferrin receptor 1, causes combined immunodeficiency*. Nat Genet, 2016. **48**(1): p. 74-8.
16. Rishi, G., D.F. Wallace, and V.N. Subramaniam, *Hepcidin: regulation of the master iron regulator*. Biosci Rep, 2015. **35**(3).
17. Beliveau, F., et al., *Discovery and Development of TMPRSS6 Inhibitors Modulating Hepcidin Levels in Human Hepatocytes*. Cell Chem Biol, 2019. **26**(11): p. 1559-1572 e9.
18. Bayeva, M., et al., *mTOR regulates cellular iron homeostasis through tristetraprolin*. Cell Metab, 2012. **16**(5): p. 645-57.
19. Guan, P. and N. Wang, *Mammalian target of rapamycin coordinates iron metabolism with iron-sulfur cluster assembly enzyme and tristetraprolin*. Nutrition, 2014. **30**(9): p. 968-74.
20. Bayeva, M., et al., *When less is more: novel mechanisms of iron conservation*. Trends Endocrinol Metab, 2013. **24**(11): p. 569-77.
21. Busti, F., et al., *Iron deficiency in the elderly population, revisited in the hepcidin era*. Front Pharmacol, 2014. **5**: p. 83.
22. Ndayisaba, A., C. Kaindlstorfer, and G.K. Wenning, *Iron in Neurodegeneration - Cause or Consequence?* Front Neurosci, 2019. **13**: p. 180.
23. Bianchi, V.E., *Anemia in the Elderly Population*. 2015. 2015.
24. Patterson, C., et al., *Iron deficiency anemia in the elderly: the diagnostic process*. CMAJ, 1991. **144**(4): p. 435-40.
25. Johnson-Wimbley, T.D. and D.Y. Graham, *Diagnosis and management of iron deficiency anemia in the 21st century*. Therap Adv Gastroenterol, 2011. **4**(3): p. 177-84.
26. Soiza, R.L., A.I.C. Donaldson, and P.K. Myint, *The pale evidence for treatment of iron-deficiency anaemia in older people*. Ther Adv Drug Saf, 2018. **9**(6): p. 259-261.
27. Bianchi, V.E., *Role of nutrition on anemia in elderly*. Clin Nutr ESPEN, 2016. **11**: p. e1-e11.

28. Vanasse, G.J. and N. Berliner, *Anemia in elderly patients: an emerging problem for the 21st century*. Hematology Am Soc Hematol Educ Program, 2010. **2010**: p. 271-5.
29. Simcox, J.A. and D.A. McClain, *Iron and diabetes risk*. Cell Metab, 2013. **17**(3): p. 329-41.
30. Verma, S. and B.J. Cherayil, *Iron and inflammation - the gut reaction*. Metallomics, 2017. **9**(2): p. 101-111.
31. Apostolakis, S. and A.M. Kypraiou, *Iron in neurodegenerative disorders: being in the wrong place at the wrong time?* Rev Neurosci, 2017. **28**(8): p. 893-911.
32. Stockwell, B.R., et al., *Ferroptosis: A Regulated Cell Death Nexus Linking Metabolism, Redox Biology, and Disease*. Cell, 2017. **171**(2): p. 273-285.
33. Jiang, H., et al., *Brain Iron Metabolism Dysfunction in Parkinson's Disease*. Mol Neurobiol, 2017. **54**(4): p. 3078-3101.
34. Belaidi, A.A. and A.I. Bush, *Iron neurochemistry in Alzheimer's disease and Parkinson's disease: targets for therapeutics*. J Neurochem, 2016. **139 Suppl 1**: p. 179-197.
35. Kaplan, C.D. and J. Kaplan, *Iron acquisition and transcriptional regulation*. Chem Rev, 2009. **109**(10): p. 4536-52.
36. Thompson, M.J., et al., *Cloning and characterization of two yeast genes encoding members of the CCCH class of zinc finger proteins: zinc finger-mediated impairment of cell growth*. Gene, 1996. **174**(2): p. 225-33.
37. Ramos-Alonso, L., et al., *Yeast Cth2 protein represses the translation of ARE-containing mRNAs in response to iron deficiency*. PLoS Genet, 2018. **14**(6): p. e1007476.
38. Ramos-Alonso, L., et al., *Iron Regulatory Mechanisms in Saccharomyces cerevisiae*. Front Microbiol, 2020. **11**: p. 582830.
39. Vergara, S.V., S. Puig, and D.J. Thiele, *Early recruitment of AU-rich element-containing mRNAs determines their cytosolic fate during iron deficiency*. Mol Cell Biol, 2011. **31**(3): p. 417-29.
40. Ramos-Alonso, L., et al., *Dissecting mRNA decay and translation inhibition during iron deficiency*. Curr Genet, 2019. **65**(1): p. 139-145.
41. Veatch, J.R., et al., *Mitochondrial dysfunction leads to nuclear genome instability via an iron-sulfur cluster defect*. Cell, 2009. **137**(7): p. 1247-58.

42. Diaz de la Loza Mdel, C., et al., *Zim17/Tim15 links mitochondrial iron-sulfur cluster biosynthesis to nuclear genome stability*. Nucleic Acids Res, 2011. **39**(14): p. 6002-15.
43. Hughes, A.L. and D.E. Gottschling, *An early age increase in vacuolar pH limits mitochondrial function and lifespan in yeast*. Nature, 2012. **492**(7428): p. 261-5.
44. Chen, K.L., et al., *Loss of vacuolar acidity results in iron-sulfur cluster defects and divergent homeostatic responses during aging in Saccharomyces cerevisiae*. Geroscience, 2020. **42**(2): p. 749-764.
45. Hughes, C.E., et al., *Cysteine Toxicity Drives Age-Related Mitochondrial Decline by Altering Iron Homeostasis*. Cell, 2020. **180**(2): p. 296-310 e18.
46. Schleit, J., et al., *Molecular mechanisms underlying genotype-dependent responses to dietary restriction*. Aging Cell, 2013. **12**(6): p. 1050-61.
47. Eide, D.J., et al., *The vacuolar H(+)-ATPase of Saccharomyces cerevisiae is required for efficient copper detoxification, mitochondrial function, and iron metabolism*. Mol Gen Genet, 1993. **241**(3-4): p. 447-56.
48. Jo, W.J., et al., *Novel insights into iron metabolism by integrating deletome and transcriptome analysis in an iron deficiency model of the yeast Saccharomyces cerevisiae*. BMC Genomics, 2009. **10**: p. 130.
49. Hu, Z., et al., *Ssd1 and Gcn2 suppress global translation efficiency in replicatively aged yeast while their activation extends lifespan*. Elife, 2018. **7**.
50. Hu, Z., et al., *Nucleosome loss leads to global transcriptional up-regulation and genomic instability during yeast aging*. Genes Dev, 2014. **28**(4): p. 396-408.
51. Lindstrom, D.L. and D.E. Gottschling, *The mother enrichment program: a genetic system for facile replicative life span analysis in Saccharomyces cerevisiae*. Genetics, 2009. **183**(2): p. 413-22, 1SI-13SI.
52. Smeal, T., et al., *Loss of transcriptional silencing causes sterility in old mother cells of S. cerevisiae*. Cell, 1996. **84**(4): p. 633-42.
53. Martinez-Pastor, M.T., A. Perea-Garcia, and S. Puig, *Mechanisms of iron sensing and regulation in the yeast Saccharomyces cerevisiae*. World J Microbiol Biotechnol, 2017. **33**(4): p. 75.
54. Gerber, A.P., D. Herschlag, and P.O. Brown, *Extensive association of functionally and cytotopically related mRNAs with Puf family RNA-binding proteins in yeast*. PLoS Biol, 2004. **2**(3): p. E79.

55. Yamaguchi-Iwai, Y., A. Dancis, and R.D. Klausner, *AFT1: a mediator of iron regulated transcriptional control in Saccharomyces cerevisiae*. EMBO J, 1995. **14**(6): p. 1231-9.
56. Ramos-Alonso, L., et al., *Molecular strategies to increase yeast iron accumulation and resistance*. Metallomics, 2018. **10**(9): p. 1245-1256.
57. Romero, A.M., et al., *Phosphorylation and Proteasome Recognition of the mRNA-Binding Protein Cth2 Facilitates Yeast Adaptation to Iron Deficiency*. mBio, 2018. **9**(5).
58. Bonawitz, N.D., et al., *Reduced TOR signaling extends chronological life span via increased respiration and upregulation of mitochondrial gene expression*. Cell Metab, 2007. **5**(4): p. 265-77.
59. Lin, S.J., et al., *Calorie restriction extends Saccharomyces cerevisiae lifespan by increasing respiration*. Nature, 2002. **418**(6895): p. 344-8.
60. Barros, M.H., et al., *Higher respiratory activity decreases mitochondrial reactive oxygen release and increases life span in Saccharomyces cerevisiae*. J Biol Chem, 2004. **279**(48): p. 49883-8.
61. Sun, N., R.J. Youle, and T. Finkel, *The Mitochondrial Basis of Aging*. Mol Cell, 2016. **61**(5): p. 654-666.
62. Mark, K.G., et al., *Ubiquitin ligase trapping identifies an SCF(Saf1) pathway targeting unprocessed vacuolar/lysosomal proteins*. Mol Cell, 2014. **53**(1): p. 148-61.
63. Li, Y., et al., *A programmable fate decision landscape underlies single-cell aging in yeast*. Science, 2020. **369**(6501): p. 325-329.
64. Curran, S.P. and G. Ruvkun, *Lifespan regulation by evolutionarily conserved genes essential for viability*. PLoS Genet, 2007. **3**(4): p. e56.
65. Smith, E.D., et al., *Quantitative evidence for conserved longevity pathways between divergent eukaryotic species*. Genome Res, 2008. **18**(4): p. 564-70.
66. Sato, T., et al., *mRNA-binding protein tristetraproline is essential for cardiac response to iron deficiency by regulating mitochondrial function*. Proc Natl Acad Sci U S A, 2018. **115**(27): p. E6291-E6300.
67. Henderson, K.A., A.L. Hughes, and D.E. Gottschling, *Mother-daughter asymmetry of pH underlies aging and rejuvenation in yeast*. Elife, 2014. **3**: p. e03504.

68. Hocine, S., et al., *Single-molecule analysis of gene expression using two-color RNA labeling in live yeast*. Nat Methods, 2013. **10**(2): p. 119-21.
69. Guldener, U., et al., *A new efficient gene disruption cassette for repeated use in budding yeast*. Nucleic Acids Res, 1996. **24**(13): p. 2519-24.
70. Ueta, R., et al., *Iron-induced dissociation of the Aft1p transcriptional regulator from target gene promoters is an initial event in iron-dependent gene suppression*. Mol Cell Biol, 2012. **32**(24): p. 4998-5008.
71. Steffen, K.K., B.K. Kennedy, and M. Kaerberlein, *Measuring replicative life span in the budding yeast*. J Vis Exp, 2009(28).
72. Lee, M.B., et al., *A system to identify inhibitors of mTOR signaling using high-resolution growth analysis in Saccharomyces cerevisiae*. Geroscience, 2017. **39**(4): p. 419-428.
73. Olsen, B., C.J. Murakami, and M. Kaerberlein, *YODA: software to facilitate high-throughput analysis of chronological life span, growth rate, and survival in budding yeast*. BMC Bioinformatics, 2010. **11**: p. 141.
74. Beaupere, C., et al., *Genome-wide quantification of translation in budding yeast by ribosome profiling*. J Vis Exp, 2017. **130**: p. e56820.
75. Chen, K., et al., *The Overlooked Fact: Fundamental Need for Spike-In Control for Virtually All Genome-Wide Analyses*. Mol Cell Biol, 2015. **36**(5): p. 662-7.
76. Dobin, A., et al., *STAR: ultrafast universal RNA-seq aligner*. Bioinformatics, 2013. **29**(1): p. 15-21.
77. Liao, Y., G.K. Smyth, and W. Shi, *The R package Rsubread is easier, faster, cheaper and better for alignment and quantification of RNA sequencing reads*. Nucleic Acids Res, 2019. **47**(8): p. e47.
78. Robinson, M.D., D.J. McCarthy, and G.K. Smyth, *edgeR: a Bioconductor package for differential expression analysis of digital gene expression data*. Bioinformatics, 2010. **26**(1): p. 139-40.
79. Anders, S. and W. Huber, *Differential expression analysis for sequence count data*. Genome Biol, 2010. **11**(10): p. R106.
80. Ritchie, M.E., et al., *limma powers differential expression analyses for RNA-sequencing and microarray studies*. Nucleic Acids Res, 2015. **43**(7): p. e47.
81. Wilcoxon, F., *Individual comparisons of grouped data by ranking methods*. J Econ Entomol, 1946. **39**: p. 269.

82. Zhang, C., *Essential functions of iron-requiring proteins in DNA replication, repair and cell cycle control*. *Protein & Cell*, 2014. **5**(10): p. 750-760.
83. Andrews, N.C., *Iron Metabolism: Iron Deficiency and Iron Overload*. *Annual Review of Genomics and Human Genetics*, 2000. **1**(1): p. 75-98.
84. Cronin, S.J.F., et al., *The Role of Iron Regulation in Immunometabolism and Immune-Related Disease*. *Frontiers in Molecular Biosciences*, 2019. **6**.
85. Hare, D., et al., *A delicate balance: Iron metabolism and diseases of the brain*. *Frontiers in Aging Neuroscience*, 2013. **5**.
86. Xu, J., et al., *Impaired Iron Status in Aging Research*. *International Journal of Molecular Sciences*, 2012. **13**(2): p. 2368-2386.
87. Shakoury-Elizeh, M., et al., *Transcriptional remodeling in response to iron deprivation in *Saccharomyces cerevisiae**. *Mol Biol Cell*, 2004. **15**(3): p. 1233-43.
88. Romero, A.M., et al., *A genome-wide transcriptional study reveals that iron deficiency inhibits the yeast TORC1 pathway*. *Biochim Biophys Acta Gene Regul Mech*, 2019. **1862**(9): p. 194414.
89. Sanvisens, N., et al., *Regulation of ribonucleotide reductase in response to iron deficiency*. *Mol Cell*, 2011. **44**(5): p. 759-69.
90. Romero, A.M., et al., *Global translational repression induced by iron deficiency in yeast depends on the *Gcn2/eIF2alpha* pathway*. *Sci Rep*, 2020. **10**(1): p. 233.
91. Young, D.J., et al., *Rli1/ABCE1 Recycles Terminating Ribosomes and Controls Translation Reinitiation in 3'UTRs In Vivo*. *Cell*, 2015. **162**(4): p. 872-84.
92. Keeling, K.M., et al., *Tpa1p is part of an mRNP complex that influences translation termination, mRNA deadenylation, and mRNA turnover in *Saccharomyces cerevisiae**. *Mol Cell Biol*, 2006. **26**(14): p. 5237-48.
93. Hausmann, A., et al., *Cellular and mitochondrial remodeling upon defects in iron-sulfur protein biogenesis*. *J Biol Chem*, 2008. **283**(13): p. 8318-30.
94. Philpott, C.C., S. Leidgens, and A.G. Frey, *Metabolic remodeling in iron-deficient fungi*. *Biochim Biophys Acta*, 2012. **1823**(9): p. 1509-20.
95. Gruschke, S., et al., *The Cbp3-Cbp6 complex coordinates cytochrome b synthesis with *bc(1)* complex assembly in yeast mitochondria*. *J Cell Biol*, 2012. **199**(1): p. 137-50.

96. Isaac, R.S., E. McShane, and L.S. Churchman, *The Multiple Levels of Mitonuclear Coregulation*. *Annu Rev Genet*, 2018. **52**: p. 511-533.
97. Lapointe, C.P., et al., *Multi-omics Reveal Specific Targets of the RNA-Binding Protein Puf3p and Its Orchestration of Mitochondrial Biogenesis*. *Cell Syst*, 2018. **6**(1): p. 125-135 e6.
98. Houshmandi, S.S. and W.M. Olivas, *Yeast Puf3 mutants reveal the complexity of Puf-RNA binding and identify a loop required for regulation of mRNA decay*. *RNA*, 2005. **11**(11): p. 1655-66.
99. Olivas, W. and R. Parker, *The Puf3 protein is a transcript-specific regulator of mRNA degradation in yeast*. *EMBO J*, 2000. **19**(23): p. 6602-11.
100. Lee, C.D. and B.P. Tu, *Glucose-Regulated Phosphorylation of the PUF Protein Puf3 Regulates the Translational Fate of Its Bound mRNAs and Association with RNA Granules*. *Cell Rep*, 2015. **11**(10): p. 1638-50.
101. Couvillion, M.T., et al., *Synchronized mitochondrial and cytosolic translation programs*. *Nature*, 2016. **533**(7604): p. 499-503.
102. Patnaik, P.K., et al., *Deficiency of the RNA-binding protein Cth2 extends yeast replicative lifespan by alleviating its repressive effects on mitochondrial function*. *Cell Rep*, 2022. **40**(3): p. 111113.
103. Zhao, X., et al., *Global identification of Arabidopsis lncRNAs reveals the regulation of MAF4 by a natural antisense RNA*. *Nat Commun*, 2018. **9**(1): p. 5056.
104. Liu, S.J., et al., *CRISPRi-based genome-scale identification of functional long noncoding RNA loci in human cells*. *Science*, 2017. **355**(6320).
105. Till, P., R.L. Mach, and A.R. Mach-Aigner, *A current view on long noncoding RNAs in yeast and filamentous fungi*. *Appl Microbiol Biotechnol*, 2018. **102**(17): p. 7319-7331.
106. Barman, P., D. Reddy, and S.R. Bhaumik, *Mechanisms of Antisense Transcription Initiation with Implications in Gene Expression, Genomic Integrity and Disease Pathogenesis*. *Noncoding RNA*, 2019. **5**(1).
107. Barre, B.P., et al., *Intragenic repeat expansion in the cell wall protein gene HPF1 controls yeast chronological aging*. *Genome Res*, 2020. **30**(5): p. 697-710.
108. Martin, M., *Cutadapt removes adapter sequences from high-throughput sequencing reads*. 2011, 2011. **17**(1): p. 3.

109. Vickers, C.E., et al., *Dual gene expression cassette vectors with antibiotic selection markers for engineering in Saccharomyces cerevisiae*. Microb Cell Fact, 2013. **12**: p. 96.
110. Miller, M.A., et al., *Carbon source-dependent alteration of Puf3p activity mediates rapid changes in the stabilities of mRNAs involved in mitochondrial function*. Nucleic Acids Res, 2014. **42**(6): p. 3954-70.
111. Patnaik, P.K., et al., *Lifespan regulation by targeting heme signaling in yeast*. Geroscience, 2024. **46**(5): p. 5235-5245.
112. Young, S.K., et al., *Ribosome Reinitiation Directs Gene-specific Translation and Regulates the Integrated Stress Response*. J Biol Chem, 2015. **290**(47): p. 28257-28271.
113. Mosca, N., A. Russo, and N. Potenza, *Making Sense of Antisense lncRNAs in Hepatocellular Carcinoma*. Int J Mol Sci, 2023. **24**(10).
114. Liu, B., et al., *The regulatory role of antisense lncRNAs in cancer*. Cancer Cell Int, 2021. **21**(1): p. 459.

CURRICULUM VITAE

